1977

Effects of heat curving on the fatigue strength of plate girders, August 1977 (DOT-FH-11.8198.5) (80-21) 67p FHWA-RD-79-136

R. P. Batcheler

J. H. Daniels

FATIGUE OF CURVED STEEL BRIDGE ELEMENTS

EFFECT OF HEAT CURVING ON THE FATIGUE STRENGTH OF PLATE GIRDERS

Submitted by

J. Hartley Daniels - Principal Investigator

R. P. Batcheler

"Prepared for the Department of Transportation, Federal Highway Administration under Contract Number DOT-FH-11-8198.

The opinions, findings and conclusions expressed in this publication are those of the authors and not necessarily those of the Federal Highway Administration."

LEHIGH UNIVERSITY
Fritz Engineering Laboratory
Bethlehem, Pennsylvania

August 1977

Fritz Engineering Laboratory Report No. 398.5

ABSTRACT

Research on the fatigue behavior of horizontally curved, steel bridge elements is underway at Lehigh University under the sponsorship of the Federal Highway Administration (FHWA) of the U. S. Department of Transportation. This multiphase investigation involves the performance of five tasks: 1) analysis and design of large scale test assemblies, 2) special studies of selected topics, 3) fatigue tests and 4) ultimate load tests of the test assemblies, and 5) development of design recommendations.

This report presents the results of a special study (Task 2) of the effects of heat curving on the fatigue strength of plate girders. The reports listed in Appendix B document other phases of this investigation.

Following a survey of the available literature on heat curving, an analytical parametric study of the residual stresses and strains due to heat curving is presented. The results of the parametric study are then examined for their applications to fatigue. Two mechanisms are considered: 1) mean stress effects on fatigue crack growth, and 2) fatigue crack growth at web boundaries due to excessive web bowing.

The results of this study indicate that heat curving has no significant effect on the fatigue strength of plate girders.

TABLE OF CONTENTS

	Page
ABSTRACT	i
LIST OF TABLES	iv
LIST OF FIGURES	v
1. INTRODUCTION	1
1.1 Description of the Heat-Curving Process	2
1.2 Development of Heat Curving	3
1.3 Objectives and Scope	4
1.4 Research Approach	5
2. DETERMINATION OF RESIDUAL STRESSES AND STRAINS DUE TO HEAT CURVING	7
2.1 Temperature Distributions during Heat Curving	7
2.2 Thermal Stress Analyses of Heat-Curved Girders	8
3. PARAMETRIC STUDY OF RESIDUAL STRESSES AND STRAINS	11
3.1 Parameters Considered	11
3.2 Results	13
3.2.1 Effects of Parameters on Radius of Curvature	13
3.2.2 Effects of Parameters on Residual Stress Distributions	14
4. APPLICATIONS TO FATIGUE	18
4.1 Effect of Mean Stress on Fatigue Crack Growth	18
4.2 Effect of Residual Stresses on Fatigue Crack Growth at Web Boundaries	21
4.2.1 Method of Analysis	22
4.2.2 Cases Considered	23
4.2.3 Results	25

Page

5. SUMMARY AND CONCLUSIONS 27

6. TABLES 29

7. FIGURES 36

8. APPENDIXES 53

54

Appendix A: Determination of Dimensionless Temperature Coefficients 54

Appendix B: List of Reports Produced under DOT-FH-11.8198 57

9. ACKNOWLEDGMENTS 58

10. REFERENCES 59

LIST OF TABLES

Table 1 Cases Analyzed in Pilot Study

Table 2 Cases Analyzed in Parametric Study

Table 3 Predicted and Minimum Allowable Radius of Curvature from Pilot Study

Table 4 Predicted and Minimum Allowable Radius of Curvature from Parametric Study

Table 5 Boundary Conditions for Finite Element Analysis of Web Boundary Problem

Table 6 Nominal Stress Range at Web Boundary from Finite Element Analysis

LIST OF FIGURES

Fig. 1(a) Plan View of Plate Girder as Fabricated by Conventional Methods

Fig. 1(b) Plan View of Plate Girder during Application of Heat (Curvature due to Nonuniform Expansion of Flanges)

Fig. 1(c) Plan View of Plate Girder after Cooling (Final Curvature due to Yielding of Heated Edges of Flanges)

Fig. 2(a) Heating Pattern for Continuous Heating Method of Heat Curving (Showing Curvature of Girder during Application of Heat)

Fig. 2(b) Heating Pattern for Wedge Heating Method of Heat Curving (Showing Curvature of Girder during Application of Heat)

Fig. 3 Dimensionless Temperature Coefficients (b_f = 24", b_h/b_f = 0.167) See Appendix A

Fig. 4 Typical Theoretical Temperature Distributions During Heat Curving (b_f = 24", b_h/b_f = 0.167, T_{max} = 1000° F)

Fig. 5 Model for Thermal Stress Analysis of Heat Curved Girders

Fig. 6 Comparison of Final Residual Stresses due to Heat Curving as Given by Missouri and U.S. Steel Analysis

Fig. 7 Effect of b_f on Radius of Curvature and Residual Stresses

Fig. 8 Effect of t_f on Radius of Curvature and Residual Stresses

Fig. 9 Effect of D_w on Radius of Curvature and Residual Stresses

Fig. 10 Effect of t_w on Radius of Curvature and Residual Stresses

Fig. 11 Effect of σ_y on Radius of Curvature and Residual Stresses

Fig. 12 Effect of b_h/b_f on Radius of Curvature and Residual Stresses

Fig. 13 Effect of T_{max} on Radius of Curvature and Residual Stresses

Fig. 14 Successive Load Cases for Web Boundary Study

Fig. 15 Finite Element Discretization for Web Boundary Study

Fig. 16 Cumulative Web Deflection for Successive Load Cases - Run 4

1. INTRODUCTION

Horizontally curved bridges are often used to simplify difficult highway alignment problems. The use of horizontally curved girders in such bridges can provide significant advantages over the use of straight girders as chords of the required curve. Curved girders are aesthetically pleasing and can substantially reduce construction costs. Curved girders allow longer span lengths, thereby reducing the number of supports, bearings, and expansion details required. Curved girders also simplify formwork for the concrete deck.[1]

One of the difficulties in the use of horizontally curved girders is the relative lack of fabrication experience. Two methods are presently used in the fabrication of curved girders. The most common method is to cut the flange plates to the required curvature and weld the web to the curved flanges. This method has two major disadvantages: 1) cutting the curved flanges from straight plates generates a large amount of scrap, and 2) special jigs are required to maintain the proper alignment of the web and flange plates during welding. The second method involves fabricating a straight girder by conventional methods and curving the girder by the application of heat to the edges of the flanges. This method is known as heat curving. Heat curving avoids the large material wastes and the requirements for special jigs inherent in the cut-to-curvature method.[1] In spite of these advantages, fabricators are slow to adopt heat curving because little information is available on the process.[2]

1.1 Description of the Heat-Curving Process

Fabrication of a horizontally curved girder by the heat-curving process begins with the fabrication of a straight girder by conventional methods as shown in Fig. 1(a).[2] Flange plates are welded to the web, and intermediate stiffeners and connection plates may be attached at the option of the fabricator.[3] Then heat is applied to the edges of the flanges which will be concave after heat curving. Due to the temperature gradient across the flanges, there is a nonuniform expansion of the flanges, causing the girder to bend in convex curvature with respect to the heated edges as shown in Fig. 1(b). If the temperature differential across the flanges is great enough, thermal axial stresses and transverse bending stresses cause compression yielding of the heated edges, developing residual strains when the girder cools. The girder, therefore, assumes concave curvature with respect to the heated edges as shown in Fig. 1(c).[2] After the girder cools completely, the radius of curvature is checked. Any necessary adjustments of the curvature may be made by subsequent applications of heat to the edges of the flanges. When the required curvature is achieved, all other details, such as longitudinal stiffeners, cover plates, gusset plates, and bearing stiffeners, are welded into place.[1]

The extent of yielding of the flanges and the resulting magnitudes of the residual strains determine the curvature of the girder. The primary means of controlling the curvature of a heat-curved girder is the appropriate selection of the maximum flange temperature and the width of the flange to be heated. In general, as the maximum heat-curving temperature and the heated width increase, the radius of curvature decreases.[2]

Several variations of the heat-curving process are in use today. These variations center on two areas: (1) the pattern in which heat is applied to the flanges and (2) the orientation of the girder during heat curving.

Two heating patterns are in current use. Heat may be applied continuously along the flanges as shown in Fig. 2(a) or at selected intervals in wedge-shaped patterns as shown in Fig. 2(b). The continuous heating method produces a smoother curve in the finished girder, particularly in very sharply curved girders. However, the wedge-heating method is more widely used. Fabricators can exercise more precise control of the resulting curvature by adjusting the distance between the wedge-shaped heating patterns. Unsightly chord effects can be avoided if the distance between the wedge-shaped heating patterns is sufficiently small.[1]

A girder may be heat curved with its web oriented vertically or horizontally. If the web is vertical during the heat-curving operation, the girder must be allowed to move laterally without turning over which requires special fixtures. If the web is horizontal during the heat-curving operation, the dead load stresses must be considered in determining the maximum temperature, the heated width and the heating pattern.[4,5] Care must also be taken to prevent inelastic buckling of the flange under dead load stresses during heating.[3]

1.2 Development of Heat Curving

The use of heat to straighten or to camber girders is common fabricating practice. Heat curving, however, is a relatively new practice which is just beginning to gain acceptance by fabricators and state transportation departments.[1]

The only systematic analytical and experimental study to date was performed by the U.S. Steel Corporation in the late 1960's.[3,6] From this study design criteria for heat-curved girders were developed.[7] These criteria were developed to prevent flange strains from exceeding acceptable limits, to control excessive web bowing, and to prevent yielding of the web under combined compression and shear loadings.[7] The criteria were subsequently adopted by various state transportation departments[3] and AASHTO.[8] United States Steel also developed fabrication aids for heat curving by the continuous heating method[4] and the wedge-heating method.[5]

No research has been reported to date on the effects of heat curving on the fatigue strength of steel plate girders.

1.3 Objectives and Scope

The primary objective of this study is to determine the effects of heat-curving on the fatigue strength of steel plate girders.

This study is part of a multiphase investigation of fatigue of curved steel bridge elements. An experimental evaluation of the effects of heat curving on fatigue strength is not feasible at this time. This report documents a preliminary, analytical investigation of the effects of heat curving on fatigue strength. Although a wide range of girder geometries and heat-curving parameters were studied, this investigation is not exhaustive. Therefore, a corollary objective of this investigation is to pinpoint areas in which more extensive analytical or experimental work should be done.

It is not the purpose of this report to document the effect of curvature per se on the fatigue strength of steel plate girders. Several forthcoming reports on work underway at Lehigh University will deal with this topic more fully.[9,10,11,12,13,14]

The primary characteristics of heat-curved girders that distinguish them from other curved girders are the residual stresses and strains produced by the heat-curving process. This study focuses on the distribution of residual stresses and strains and their effects on the fatigue strength of heat-curved steel plate girders. Consideration is given to the problems of web boundary cracking and mean stress effects on fatigue crack growth.

1.4 Research Approach

This study consists of four major phases:

First, a literature survey on heat curving was conducted. The results are summarized in the preceding articles.

Second, the variation of temperature throughout the heat-curving process was determined. A satisfactory approximation of this variation is obtained from the principles of heat transfer in thin, semi-infinite plates as outlined in Article 2.1 and Appendix A.[2,15,16]

Third, the residual stresses and strains produced by heat curving were determined by nonlinear thermal stress analysis.[17] The temperature distributions obtained in the second phase define the thermal loading at

given time increments. The thermal stress analysis is outlined in Article 2.2 and the results are reported in Chapter 3.

Fourth, the results of the thermal stress analyses were examined for their applications to fatigue. Specifically, the residual stresses and strains produced by heat curving are examined for possible effects on fatigue crack growth. Two primary mechanisms are considered: (1) fatigue crack growth at the flange-web boundary, and (2) mean stress effects on fatigue crack growth. Chapter 4 outlines this phase of the study.

The report closes with conclusions and recommendations for further study.

2. DETERMINATION OF RESIDUAL STRESSES AND STRAINS DUE TO HEAT CURVING

2.1 Temperature Distributions during Heat Curving

The residual stresses and strains produced by heat curving are determined by thermal stress analyses of girders curved through application of different maximum temperatures over various heated widths. The thermal stress analyses assume an elastic-perfectly plastic stress-strain response and temperature dependent material properties. The results of such analyses are path-dependent. That is, the results depend on the magnitude and sequence of the thermal loadings. Therefore, the variation of temperature over the girder cross section must be known throughout the heat-curving process.[17]

In order to simplify the thermal stress analyses it is assumed the continuous variation of temperature during heat curving is satisfactorily approximated by the temperature distributions at six discrete time intervals. A similar approach by Brockenbrough predicted the residual stresses and strains due to heat curving within an acceptable degree of error.[2]

Determination of the required temperature distributions is based upon the principles of heat transfer in a thin, semi-infinite plate. The temperature at a given point on the flange is a function of the heat input, the position of the point relative to the moving heat source, and various thermal properties of the flange plate.[15,16]

The temperature, T_{ij}, at a given point, i, for a given time increment, j, is determined from:

$$T_{ij} = T_o + k_{ij} \Delta T \qquad (2\text{-}1)$$

where T_o = the ambient temperature

k_{ij} = a dimensionless temperature coefficient, unique to the point, i, for the time increment, j

ΔT = the difference between the maximum heat-curving temperature and the ambient temperature.

Figure 3 shows the dimensionless temperature coefficients, k_{ij}, obtained for a flange width, b_f, of 24 inches and a heated width, b_h, of 4 inches. Determination of the dimensionless temperature coefficients is detailed in Appendix A.

Figure 4 shows the resulting theoretical temperature distributions for a flange width, b_f, of 24 inches, a heated width, b_h, of 4 inches, ad a maximum heat-curving temperature, T_{max}, of 1000°F. Reasonable agreement between the theoretical temperature distributions used in this investigation and the limited information available on actual temperature distributions during heat curving was obtained.

2.2 Thermal Stress Analyses of Heat-Curved Girders

With the temperature distributions known from the procedure outlined in Article 2.1 the thermal stress analyses of heat-curved girders can be carried out. The thermal stress analyses are performed using a computer program written at the University of Missouri. In this program the girder to be analyzed is modeled as a collection of discrete elements. The model consists of 13 elements as shown in Fig. 5. The temperature of each element for a given time increment is the temperature at the centroid of the element.[17]

Following the input of girder properties, locations of elements and temperature distributions for the time increments under study, the computer program begins with the first time increment and determines the distribution of stresses and strains at a cross section subject to the given temperature. This is accomplished as follows:

1. A trial value of the uniform strain and curvature at the cross section is selected for the given temperature distribution.
2. The stress on each element is calculated from the strains given by step 1.
3. The net unbalanced axial force and bending moment are determined by summation.
4. Iteration is used to adjust the assumed value of the uniform strain to achieve force equilibrium at the cross section.
5. Iteration of the uniform strain and curvature are employed to achieve both force and moment equilibrium.
6. Print the results and continue to the next time increment.

The stresses, strains, and temperature distributions from the preceding time increment describe the reference state for each successive time increment. The temperature dependence of the yield strength, Young's modulus, and the coefficient of thermal expansion, as well as an assumed elastic-perfectly plastic stress-strain response, are included in the analysis.[17]

The applicability of this analysis to the bending of beams under thermal loads was demonstrated in an investigation of flame cambering.[17] Analysis of several girders tested in the theoretical and experimental investigation of heat curving carried out at U.S. Steel shows good agreement between the results of the Missouri program and those obtained at U.S. Steel. Figure 6 shows a comparison of the residual stresses obtained by U.S. Steel to those given by the Missouri computer program

for one of the girders included in the U.S. Steel investigation.[2] In Fig. 6 σ_{rf} is the final residual stress in the flange due to heat curving, and σ_{rw} is the final residual stress in the web. A positive residual stress denotes tension for both σ_{rf} and σ_{rw}.

3. PARAMETRIC STUDY OF RESIDUAL STRESSES AND STRAINS

3.1 Parameters Considered

Eighteen pilot cases based on the girder geometries and temperature distributions of the U.S. Steel study are shown in Table 1. These cases were used to evaluate the applicability of the Missouri program to the analysis of heat-curved girders and to assist in identifying the significant parameters which should be studied. Following the analysis of these pilot cases and an evaluation of the results, a more complete parametric study was established as shown in Table 2.

The parameters chosen for study relate to the geometric and material properties of the girder and to the heat-curving process. These parameters include:

a. the width of the flanges, b_f

b. the thickness of the flanges, t_f

c. the depth of the web, D_w

d. the thickness of the web, t_w

e. the ratio of the total cross-sectional area of the girder to the area of both flanges, Ψ

f. the desired radius of curvature, R

g. the material yield strength, σ_y

h. the ratio of the heated width of the flanges, b_h, to the total width of the flanges, b_f, and

i. the maximum heat-curving temperature, T_{max}.

The ranges of the parameters chosen for study represent practical extremes of each parameters as follows:

a. A flange width of 6 inches is a practical minimum width. A flange width of 30 inches is the maximum for which heat curving is permitted by AASHTO without special provisions.[8] Intermediate values of 12 and 24 inches are considered.

b. Similar comments apply to the selection of 0.5 inches and 3.0 inches as the minimum and maximum flange thicknesses, respectively.[8] Intermediate values of 1.0 and 2.0 inches are also considered.

c. The web depth varies from 36 inches to 96 inches with intermediate values of 48 inches and 60 inches. This seems a practical range of web depths.

d. Similar reasoning establishes the range of web thicknesses as 0.25 inches, 0.50 inches, and 0.75 inches.

e. The ratio of the total cross-sectional area of the girder to the area of both flanges, Ψ, is, of course, dependent on the preceding parameters. No attempt was made to control Ψ independently of the preceding parameters. A range of values of Ψ from 1.25 to 3.50 is included in the study.

f. The radius of curvature cannot be controlled independently of the other parameters, therefore its effect will be determined by a review of all cases run.

g. The material yield strength varies between 36 ksi (A36 steel) and 50 ksi (A588 steel). Heat curving of girders fabricated from steels with specified minimum yield strengths greater than 50 ksi is not permitted.[3,8]

h. The ratio of the heated width to the total width of the flange ranges from 0.083 to 0.500. The lower value represents a practical minimum value, and the higher value approaches 0.625, the maximum allowed by AASHTO for the wedge-heating method.[8]

i. The maximum heat-curving temperature is either 800°F or 1100°F. The results of the U.S. Steel study indicate that below 800°F very little curvature results from heat-curving.[2,6] Heating a girder above 1200°F during heat curving is not permitted due to possible effects on mechanical and material properties.[3,8]

3.2 Results

3.2.1 Effects of Parameters on Radius of Curvature

The final radius of curvature, R_{est}, predicted by the thermal stress analysis described in Chapter 2 is shown in Tables 3 and 4 for each case studied.

The AASHTO Specifications limit the minimum radius of curvature for heat-curved girders. These limits are expressed by equations developed in the U.S. Steel study as follows:

$$R_{min} \geq 150 \text{ ft} \tag{3-1}$$

$$R_{min} \geq \frac{1.167}{\sqrt{\sigma_y}} \frac{b_f}{\Psi} \frac{D_w}{t_w} \tag{3-2}$$

$$R_{min} \geq \frac{625}{\sigma_y} \frac{b_f}{\Psi} \tag{3-3}$$

The governing value of R_{min} is given by Eqs. 3-1, 3-2, or 3-3, whichever is greater.[3,7,8] The governing value of R_{min} is shown in Tables 3

and 4 for each case studied. Only cases 9, 19, 21, 30, and 31 violate these provisions.

In general, the effects of the various parameters on the radius of curvature are as follows:

1. As b_f or t_f increase, R increases. As D_w or t_w increase, R decreases.

2. Since Ψ is inversely proportional to b_f and t_f, and directly proportional to D_w and t_w, it is possible to extend observations on b_f, t_f, D_w, and t_w to Ψ. As Ψ increases, R decreases.

3. As σ_y increases, R increases.

4. As b_h/b_f increases, R decreases.

5. As T_{max} increases, R decreases.

The above generalizations apply to all cases studied with the exception of the statement regarding the effect of b_h/b_f on the radius of curvature. In cases 39, 42, and 45 (Tables 2 and 4), the radius of curvature increases when b_h/b_f equals 0.500. This is attributed to the uniform axial strain of the girder which increases markedly when a large portion of the flange is subjected to T_{max}. This uniform axial strain does not contribute to the final radius of curvature of the girder.

3.2.2 Effects of Parameters on Residual Stress Distributions

The residual stress distributions for a number of selected cases are shown in Figures 7 through 13. The residual stress distributions

are constructed from the results of the thermal stress analyses of heat-curved girders (Art. 2.2).

In Figs. 7 through 13, the ordinate, σ_{rf}, is the residual stress in the flange after heat curving. The sign convention employed is positive denotes a tensile residual stress and negative denotes a compressive residual stress . The residual stresses shown are the values given by the thermal stress analyses for the centroid of each element across the flange width (Fig. 5). The abscissa indicates the location of the centroid of each element relative to the centerline of the flange in inches. The positive direction is away from the heated edge of the flange, that is, away from the final center of curvature. Conversely, the negative direction is toward the heated edge of the flange, that is, toward the final center of curvature. Below each figure is a key to permit identification of each residual stress distribution by the corresponding case number (Tables 1 and 2). Below the key are the parameters common to all cases shown in the figure. The parameter which is being varied in each figure is shown in the third column of the key along with the values it assumes for each case shown. The radius of curvature, R, and the residual stress in the web, σ_{rw}, after heat curving are shown in the last two columns of the key.

The residual stress distributions for Cases 19 through 22 are shown in Fig. 7, illustrating the effects of various flange widths. Figure 8 shows residual stress distributions for Cases 23 through 26 and the effects of various flange thicknesses. Figure 9 (Cases 27 through 30) and Figure 10 (Cases 31 through 33) illustrate the effects of various web depths and thicknesses, respectively.

Careful inspection of Figures 7 through 10 shows the geometric properties of the girder have little significant effect on the final residual stress distribution across the flange width. The compressive residual stress in the web increases, however, as b_f or t_f increase, or as D_w or t_w decrease. The compressive residual stress in the web, therefore, increases as Ψ decreases.

Since any particular final radius of curvature may be obtained by many different combinations of other parameters, the relationship between the radius of curvature and the residual stresses produced by heat curving is inconclusive.

The shape of the residual stress distribution does not change significantly with an increase in material yield strength as shown in Figure 11 (Cases 35 and 41). The peak values of the residual stresses increase markedly, however, with increases in σ_y. The compressive residual stress in the web decreases as σ_y increases.

The most significant changes in the residual stresses occur with the parameters which characterize the heat-curving process, i.e., the ratio b_h/b_f, and the maximum heat curving temperature, T_{max}. As the ratio b_h/b_f increases, the peak value of the tensile residual stress moves toward the center of the flange as shown in Figure 12. The compressive residual stress in the web also increases significantly. Most importantly, particularly with regard to fracture, the tensile residual stresses extend across an increasingly large portion of the width of the flange as b_h/b_f increases.

Finally, the peak value of the tensile residual stresses decreases rapidly as T_{max} decreases as shown in Figure 13 (Cases 35 and 38). Corresponding decreases in the compressive residual stresses in the web occur as T_{max} decreases.

4. APPLICATIONS TO FATIGUE

As noted earlier, the primary characteristics of heat-curved girders that distinguish them from other curved girders are the residual stresses and strains produced by the heat-curving process. The search for a mechanism (or mechanisms) whereby these residual stresses and strains might have a significant effect upon the fatigue strength of heat-curved girders constitutes a major portion of this study.

After an extensive literature survey and review of previous research on fatigue of structural steel bridge members, two possible mechanisms require particular study. These possible mechanisms are:

1. the direct effect of the residual stresses on fatigue strength through mean stress effects on fatigue crack growth, and
2. the indirect effect of the residual stresses on fatigue strength through fatigue crack growth at the web boundaries.

4.1 Effect of Mean Stress on Fatigue Crack Growth

Extensive analytical and experimental evidence establishes the range in the stress intensity, ΔK, as the primary parameter controlling fatigue crack propagation. Paris and Erdogan observed that the fatigue crack growth rate, $\frac{da}{dN}$, is related to ΔK by the equation:

$$\frac{da}{dN} = C\ (\Delta K)^n \qquad (4\text{-}1)$$

where C and n are empirical constants for the given material and environmental conditions.[18,19]

For a crack of a given length, a, ΔK is given by:

$$\Delta K = CF * S_r\sqrt{\pi a} \qquad (4\text{-}2)$$

where S_r is the nominal stress range and CF is a correction factor including the effects of front and back free surfaces, crack shape, and nonuniform stress distributions. Rearranging Eq. 4-1, integrating, and dividing through by $(S_r)^n$ gives the number of cycles, N, required to propagate a crack from an initial crack length, a_i, to some final crack length, a_f:

$$N = \left[\frac{1}{C}\int_{a_i}^{a_f} \frac{1}{(\Delta K/S_r)^n}\, da\right] S_r^{-n} = AS_r^{-n} \qquad (4\text{-}3)$$

Substituting Eq. 4-2 into Eq. 4-3 and given the constants, C and n, the parameter, A, can be evaluated and a fatigue life estimate obtained.[20]

Equation 4-3 demonstrates an important point. The stress state at a particular detail affects the fatigue strength of the detail only in terms of the stress range. The mean stress level (whether due to dead loads, residual stresses or other causes) does not significantly affect the fatigue life of the detail.[21,22,23,24]

The important exceptions to the mean stress independence of fatigue crack growth should be noted. The first exception occurs when the mean stress is such that the stress range takes place entirely within a compressive stress cycle. If both the minimum and maximum stresses are compressive, no crack opening displacement and, therefore, no fatigue crack growth, can occur. This observation explains the results of a number of fatigue tests of steel beams in which fatigue failure occurred in the tension flange, while no significant fatigue crack growth was observed in the compression flanges even though the stress ranges were identical. Although analysis may indicate that

a stress range takes place entirely within a compressive stress cycle, superposition of tensile residual stresses may produce a stress range which, in whole or in part, experiences a tensile stress excursion. Such tensile residual stress fields exist in the vicinity of welded structural details, therefore fatigue crack growth can take place even under a compressive stress range. Such tensile residual stresses decay rapidly, however, and fatigue crack growth arrests as the crack grows out of the influence of the tensile residual stresses. This behavior has been observed experimentally in a large number of tests.[21]

The existence of tensile residual stresses across a large portion of the flange width of a heat-curved girder as indicated in Chapter 3 implies that fatigue cracks could grow to significant sizes even under compressive stress ranges. If any stress reversal is observed in the stress cycle the possibility of fracture exists. In any case it is conservative to assume the entire stress range is effective in promoting fatigue crack growth. In light of the extensive tensile residual stresses generated by heat curving this assumption seems particularly prudent.

The second exception to the mean stress independence of fatigue crack propagation involves modification of the Paris fatigue crack growth relationship of Eq. 4-1. Various revised fatigue crack growth relationships are available in the current fracture mechanics literature. One of the revised relationships most often advanced is:

$$\frac{da}{dN} = \frac{C(\Delta K)^n}{(1-R)(K_c-\Delta K)} \qquad (4-4)$$

where R is the ratio of the minimum stress intensity to the maximum stress intensity, K_c is the fracture toughness, or critical stress

intensity, of the given material and detail geometry, and C and n are empirical constants as in Eq. 4-1. This relationship reflects the contribution of static modes of crack growth.[25]

For common structural steels of moderate strength and high toughness the contributions of static modes of crack growth are negligible for rates of fatigue crack growth less than 10^{-4} in./cycle.[26] Similar comments can be made with regard to other proposed revisions of the Paris fatigue crack growth relationship.[25,26] In short, for the materials and crack growth rates normally anticipated in highway bridges the effects of mean stress levels on the fatigue crack growth rate are negligible.

Results from a number of experimental studies bear out the conclusion that mean stress levels and, therefore, residual stresses, have a negligible effect on fatigue crack growth for the materials and stress conditions of interest in the fatigue of steel highway bridges.[21,22,24] Of particular interest are the results of experimental programs carried out by Gurney[23] and Fisher.[21,22] Both experimental studies showed no significant effect of mean stress levels or residual stresses on fatigue crack growth.

4.2 Effect of Residual Stresses on Fatigue Crack Growth at Web Boundaries

Equations 3-2 and 3-3 (Art. 3.2.1) are included in the AASHTO Specifications in order to limit the compressive residual stresses developed in the webs of heat-curved girders. The results of the preceding analyses showed, however, that compressive residual stresses as high as 28.7 ksi (Fig. 7) can be developed in the webs of heat-curved

girders conforming to the requirements of Eqs. 3-1 through 3-3. The possibility that these compressive residual stresses may generate excessive web deformations and thereby cause fatigue crack growth at the web boundaries should be considered.[27]

It is not the intention of this work to present a complete parametric study of fatigue crack growth at web boundaries of heat-curved girders. The approach taken in this study is to analyze several severe test cases to establish whether or not fatigue crack growth at the web boundaries is likely to be a problem.

4.2.1 Method of Analysis

Analysis of the out-of-plane behavior of a web panel under in-plane forces is normally a very complex problem involving stability considerations. In the case of a curved web panel of a relatively small radius of curvature, however, it is possible to simplify the analysis by considering the panel to be a grossly imperfect plate. Out-of-plane displacements of an imperfect plate under in-plane forces take the form of the imperfections. In the case of a curved web panel, longitudinal stresses merely increase or decrease the initial curvature of the panel depending upon whether the stresses are compressive or tensile. A second-order elastic analysis will satisfactorily model this behavior in the elastic range. A true second-order elastic analysis of a curved web panel is very difficult. In order to simplify the analysis it is assumed that the second-order behavior of the curved web panel is satisfactorily represented by an incremental first-order analysis. This is done in three steps as indicated in Fig. 14. First, the web panel is analyzed to determine the deflected shape of the panel under the action

of the residual stresses. This deflected shape is used as the original configuration of the web panel for its analysis under dead load stresses. Similarly, the deflected shape of the panel under dead load stresses becomes the original configuration for the analysis of the web panel under live load. The resulting moments at the web boundaries are divided by the section modulus of a unit width strip of the web to yield nominal stress ranges at the web boundaries.

The first-order analysis of the web panel under each successive load case is carried out by a finite element analysis using SAP IV.[28] Taking advantage of the assumed symmetry of the web panel and loading about mid-panel permits the use of the finite element discretization shown in Fig. 15. The model is composed of 40 thin plate/shell elements and 54 nodes, comprising 236 degrees of freedom. The mesh is graded slightly toward the region of interest at mid-panel. The loads indicated in Fig. 14 are imposed by specifying displacements corresponding to the elastic strains at each node along sides a, b, and d. The boundary conditions for the finite element model differ slightly between the various cases considered.

4.2.2 Cases Considered

A total of five test runs are presented. In all runs the depth of the web is 60 inches. The length of the web panel is also 60 inches for an aspect ratio of 1.0. The radius of curvature is 150 feet. The applied stresses chosen for the analysis of web boundary stresses are constant for all five test runs. The residual compressive stress in the web is 25 ksi as shown in Fig. 14. The maximum dead load bending and the maximum live load bending stresses are 10 ksi (Fig. 14). The

indicated differences in the distribution of dead load and live load stresses through the depth of the steel section reflect the consideration given to the probable construction sequence and assumed composite action. The primary differences between the 5 test runs lie in the choice of web slenderness ratios and boundary conditions for the finite element analysis.

Review of a survey by the FHWA[9] shows the mean value of the web slenderness ratio of a number of existing curved girder bridges is 147 with a standard deviation of 54. The web slenderness ratios chosen for the study are 147, 201, and 93 which correspond to the mean value, the mean value plus one standard deviation, and the mean value minus one standard deviation. The corresponding web thicknesses for the test runs are 0.471, 0.644, and 0.299 inches. Test Runs 2, 4, and 5 have web thicknesses of 0.471 inches. Run 1 has a web thickness of 0.299 inches. The web thickness for Run 3 is 0.644 inches.

The boundary conditions for the finite element analysis are shown in Table 5. Referring to Fig. 15, the boundary conditions for Runs 1, 2, and 3 represent the following assumptions:

1. Symmetry about mid-panel (side c)
2. The complete effectiveness of the diaphragm and transverse stiffeners in resisting distortion of the cross section (side b), and
3. The complete fixity of the web due to the restraint of the composite slab and bottom flange (sides a and d).

In Runs 4 and 5 the boundary conditions were modified to reflect the partial fixity of the bottom edge of the web. Instead of fixing side d against displacement in the radial direction and rotation about the tangential axis as in Runs 1 through 3, beam elements were added along

side d to represent the bottom flange. This allows the effects of flange raking and the rotation of the bottom flange on web boundary stresses to be included in the analysis.

The residual stress load case is not included in the analysis of Run 5. Comparison of Runs 4 and 5 permit the effect of web bowing under compressive residual stresses on the stress range at the web boundary to be evaluated.

4.2.3 Results

The maximum nominal stress ranges at the web boundaries for Runs 1 through 5 are shown in Table 6. Comparison of Runs 1, 2, and 3 shows that the intermediate web thickness is the governing case. This is reasonable in light of the fact that the stress range at the web boundary is not strictly displacement- or stress-controlled.

Comparison of Runs 2 and 4 shows the significant contribution of flange raking to the stress range at the web boundary. Similarly, this comparison demonstrates the insignificance of the relaxation of web boundary stresses due to rotation of the bottom flange relative to the increase in web boundary stresses due to flange raking.

Comparison of Runs 4 and 5 shows the increase in the stress range at the web boundary due to web bowing under compressive residual stresses.

The maximum web boundary stress range, 11.2 ksi, occurs for Run 4. If the fatigue strength of the web-to-flange juncture is assumed equivalent to that of a stiffener (AASHTO Category C) the maximum web boundary stress range is below the fatigue life runout.[29] Therefore, fatigue crack growth at the web boundaries should not be a significant problem.

Consideration of the following three factors indicate that this conclusion is probably valid for any heat-curved girder conforming to current AASHTO and AWS Specifications.

First, the cases studied represent an extreme with regard to web bowing due to the combination of the minimum allowable radius of curvature for heat-curved girders (150 feet) and very high compressive residual stresses in the web (25 ksi). Also the live load bending stress range of 10 ksi is a reasonable maximum for the R.M.S. live load bending stress range.[30]

Second, the method of analysis assumes that the compressive residual stresses act on the web in its final curved configuration. In reality, the residual stresses increase simultaneously with the curvature of the girder as it cools. An incremental analysis that reflects this simultaneous development would be more accurate and would probably predict far less web bowing.

Third, the web deflection concerns the AWS web flatness requirements. The deflected shape of the web is shown for Run 4 in Fig. 16. Also shown is the AWS limit on web bowing of $D_w/150$.[31] The web deflection under the action of residual stresses only (i.e., after heat curving) exceeds the AWS limit. If the web bowing is restricted to the AWS limit, the stress range at the web boundary would be even lower.

5. SUMMARY AND CONCLUSIONS

A study of the effects of heat curving on the fatigue strength of plate girders is presented. The study focuses on the effects of the residual stresses and strains produced by heat curving on fatigue strength.

The report begins with a parametric study of the residual stresses and strains produced by heat curving. The effects of parameters relating to the geometric and material properties of the girder and to the heat-curving process are shown in Chapter 3.

An analysis of the results of the parametric study seeks the effects of these residual stresses on fatigue strength. Two primary mechanisms are studied:

1. Mean stress effects on fatigue crack growth, and
2. Fatigue crack growth at web boundaries due to excessive web bowing under compressive residual stresses.

Heat curving has no significant effect on the fatigue strength due to either mechanism.

Two recommendations should be made with regard to the fatigue of heat-curved girders:

1. If any stress reversal occurs, the entire stress range (including compressive stress excursions) should be considered effective in promoting fatigue crack growth in the flanges of heat-curved girders, and

2. The existing AWS web flatness requirements should be strictly applied to curved girders after heat curving.

Recommendations for further study include:

1. Experimental verification of the negligible effects of heat curving on the fatigue strength of plate girders,

2. Study of the influence of heat curving on fracture resistance, and

3. Further study of the possibility of fatigue crack growth at web boundaries to verify the conservativeness of the conclusions of this study with regard to the web boundary problem.

6. TABLES

TABLE 1 - CASES ANALYZED IN PILOT STUDY

Case	b_f (inches)	t_f (inches)	D_w (inches)	t_w (inches)	b_h/b_f (-)	T_{max} ($^{\circ}F$)	σ_y (ksi)
1	24	1.0	46	0.50	0.083	800	36
2	24	1.0	46	0.50	0.167	800	36
3	24	1.0	46	0.50	0.250	800	36
4	24	1.0	46	0.50	0.083	1100	36
5	24	1.0	46	0.50	0.167	1100	36
6	24	1.0	46	0.50	0.250	1100	36
7	24	2.0	46	0.50	0.083	800	36
8	24	2.0	46	0.50	0.167	800	36
9	24	2.0	46	0.50	0.250	800	36
10	24	2.0	46	0.50	0.083	1100	36
11	24	2.0	46	0.50	0.167	1100	36
12	24	2.0	46	0.50	0.250	1100	36
13	24	3.0	46	0.50	0.083	800	36
14	24	3.0	46	0.50	0.167	800	36
15	24	3.0	46	0.50	0.250	800	36
16	24	3.0	46	0.50	0.083	1100	36
17	24	3.0	46	0.50	0.167	1100	36
18	24	3.0	46	0.50	0.250	1100	36

TABLE 2 - CASES ANALYZED IN PARAMETRIC STUDY

Case	b_f (inches)	t_f (inches)	D_w (inches)	t_w (inches)	b_h/b_f (-)	T_{max} (°F)	σ_y (ksi)
19	6	2.0	60	0.50	0.250	1100	36
20*	12	2.0	60	0.50	0.250	1100	36
21	24	2.0	60	0.50	0.250	1100	36
22	30	2.0	60	0.50	0.250	1100	36
23	12	0.5	60	0.50	0.250	1100	36
24	12	1.0	60	0.50	0.250	1100	36
25*	12	2.0	60	0.50	0.250	1100	36
26	12	3.0	60	0.50	0.250	1100	36
27	12	2.0	36	0.50	0.250	1100	36
28	12	2.0	48	0.50	0.250	1100	36
29*	12	2.0	60	0.50	0.250	1100	36
30	12	2.0	96	0.50	0.250	1100	36
31	12	2.0	60	0.25	0.250	1100	36
32*	12	2.0	60	0.50	0.250	1100	36
33	12	2.0	60	0.75	0.250	1100	36
34	12	2.0	60	0.50	0.167	1100	36
35*	12	2.0	60	0.50	0.250	1100	36
36	12	2.0	60	0.50	0.500	1100	36
37	12	2.0	60	0.50	0.167	800	36
38	12	2.0	60	0.50	0.250	800	36
39	12	2.0	60	0.50	0.500	800	36
40	12	2.0	60	0.50	0.167	1100	50
41	12	2.0	60	0.50	0.250	1100	50
42	12	2.0	60	0.50	0.500	1100	50
43	12	2.0	60	0.50	0.167	800	50
44	12	2.0	60	0.50	0.250	800	50
45	12	2.0	60	0.50	0.500	800	50

*Cases are identical; included to facilitate comparison

TABLE 3 - PREDICTED AND MINIMUM ALLOWABLE RADIUS OF CURVATURE FROM PILOT STUDY

Case	R_{est} (feet)	R_{min} (feet)
1	4083.	290.3
2	1839.	290.3
3	939.3	290.3
4	2013.	290.3
5	735.9	290.3
6	367.8	290.3
7	4525.	346.4
8	1223.	346.4
9	101.9	346.4
10	2178.	346.4
11	685.6	346.4
12	381.0	346.4
13	4532.	370.2
14	1258.	370.2
15	1238.	370.2
16	2226.	370.2
17	771.5	370.2
18	386.9	370.2

TABLE 4 - PREDICTED AND MINIMUM ALLOWABLE RADIUS OF CURVATURE FROM PARAMETRIC STUDY

Case	R_{est} (feet)	R_{min} (feet)
19	78.72	150.0
20	190.2	172.3
21	376.7	426.7
22	3199.	560.0
23	156.3	150.0
24	168.5	150.0
25	190.2	172.3
26	204.4	197.6
27	209.7	151.5
28	197.8	150.0
29	190.2	172.3
30	174.4	224.0
31	217.9	426.7
32	190.2	172.3
33	176.6	150.0
34	261.6	172.3
35	190.2	172.3
36	173.4	172.3
37	745.7	172.3
38	690.4	172.3
39	1985.	172.3
40	375.3	150.0
41	303.4	150.0
42	304.8	150.0
43	6161.	150.0
44	4782.	150.0
45	6816.	150.0

TABLE 5 - BOUNDARY CONDITIONS FOR FINITE ELEMENT ANALYSIS OF WEB BOUNDARY PROBLEM (see Fig. 15)

Displacements in:	Runs 1,2,3				Runs 4,5			
	Side a	Side b	Side c	Side d	Side a	Side b	Side c	Side d
Vertical Direction	S				S			
Radial Direction	S	S		S	S	S		
Tangential Direction	G	G	S	G	G	G	S	G
Rotations About:								
Vertical Axis	S	S	S		S	S	S	
Radial Axis	S[a]	S[a]	S[a]	S[a]	S[a]	S[a]	S[a]	S[a]
Tangential Axis	S	S		S	S	S		

Key:

(Blank) = Free

G Given by specified loading condition

S Stopped

[a] Rotation about radial axis must be stopped at all nodes to provide stiffness to rotation about axes normal to the plane of the element.

TABLE 6 - NOMINAL STRESS RANGE AT WEB BOUNDARY FROM FINITE ELEMENT ANALYSIS

Run	t_w (inches)	S_r (ksi)
1	0.298	9.23
2	0.471	9.38
3	0.644	7.75
4[a]	0.471	11.21
5[ab]	0.471	6.18

[a]Include effects of flange raking and rotation

[b]No compressive residual stress in web

7. FIGURES

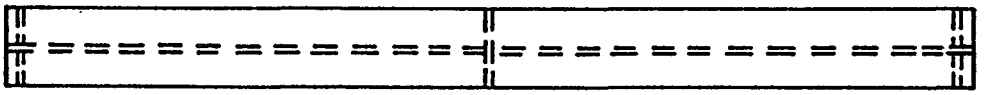

Fig. 1(a) Plan View of Plate Girder as Fabricated by Conventional Methods

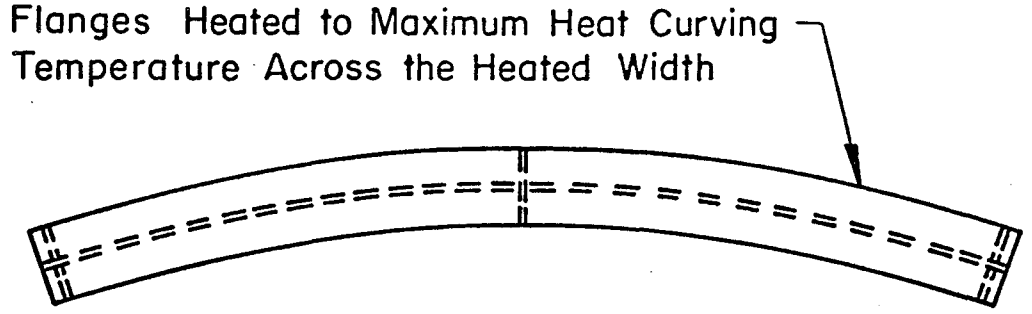

Fig. 1(b) Plan View of Plate Girder during Application of Heat (Curvature due to Nonuniform Expansion of Flanges)

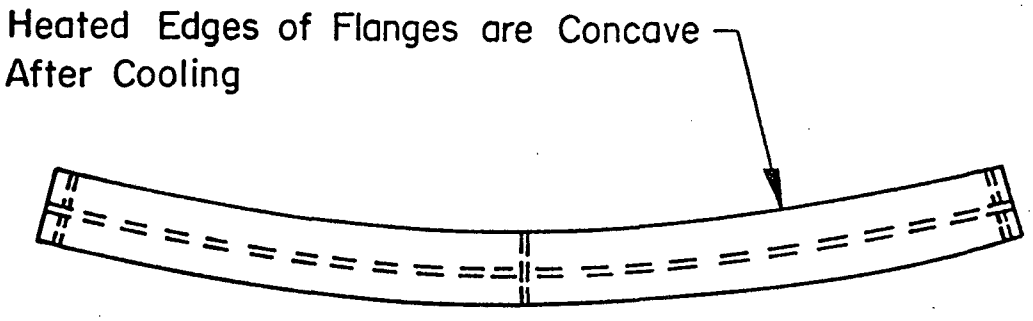

Fig. 1(c) Plan View of Plate Girder after Cooling (Final Curvature due to Yielding of Heated Edges of Flanges)

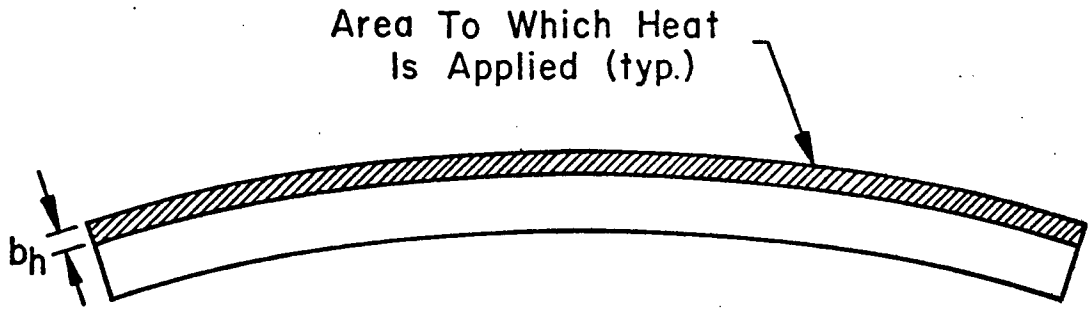

Fig. 2(a) Heating Pattern for Continuous Heating Method of Heat Curving (Showing Curvature of Girder during Application of Heat)

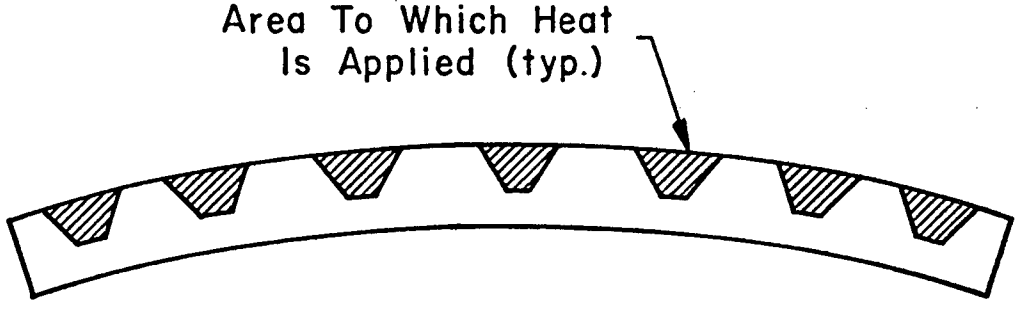

Fig. 2(b) Heating Pattern for Wedge Heating Method of Heat Curving (Showing Curvature of Girder during Application of Heat)

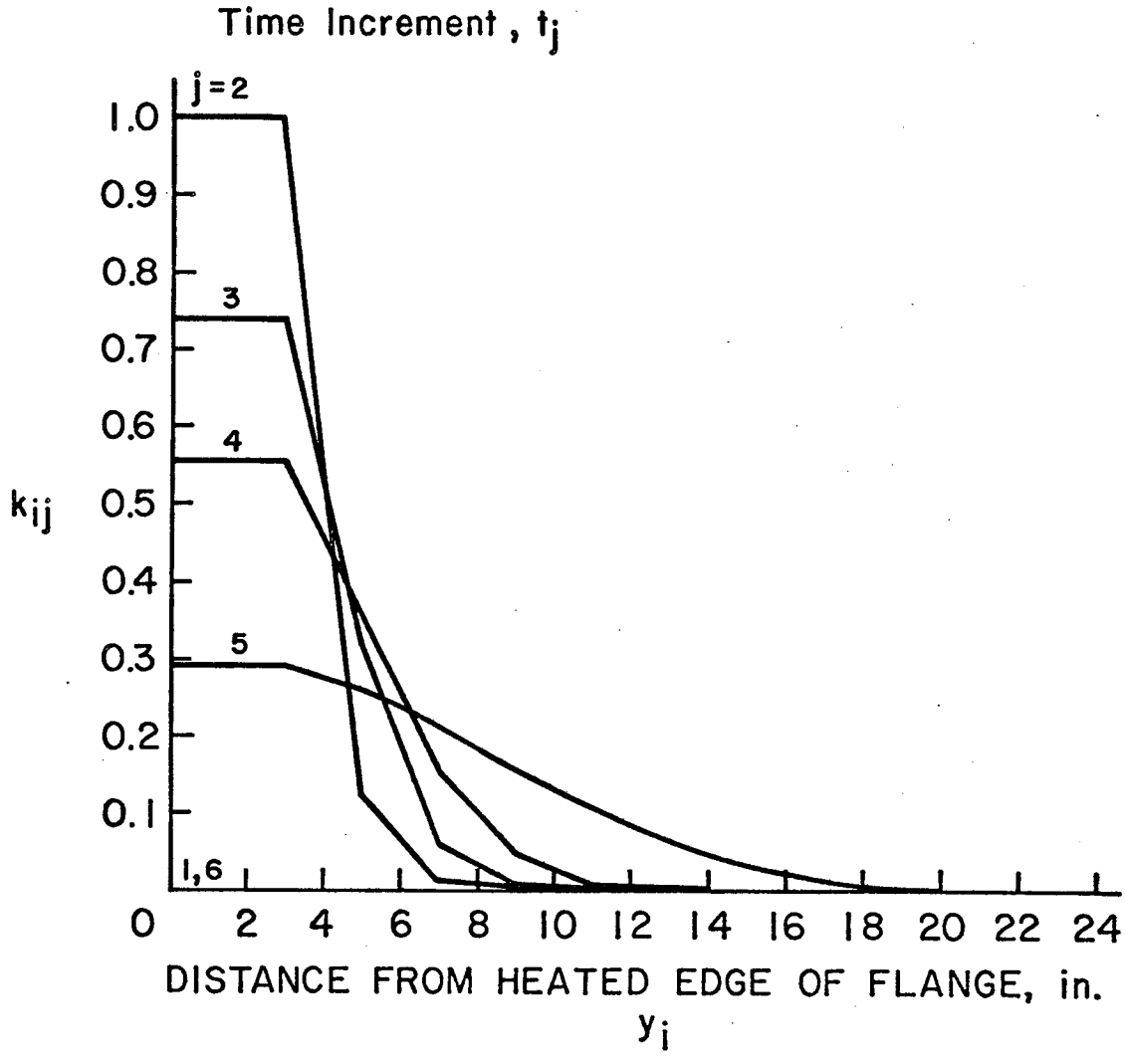

Fig. 3 Dimensionless Temperature Coefficients (b_f = 24", b_h/b_f= 0.167) See Appendix A

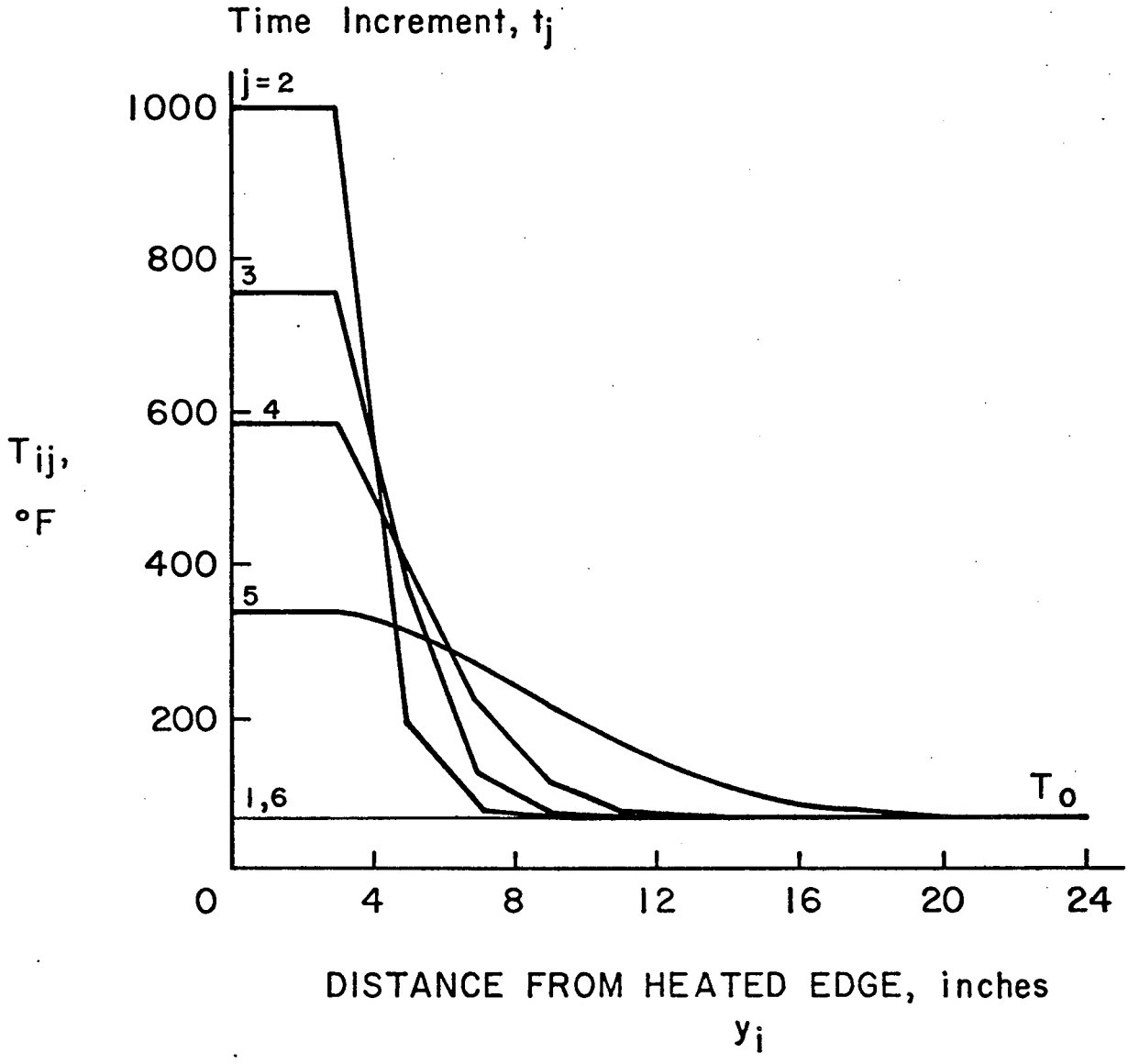

Fig. 4 Typical Theoretical Temperature Distributions During Heat Curving (b_f = 24", b_h/b_f = 0.167, T_{max} = 1000° F)

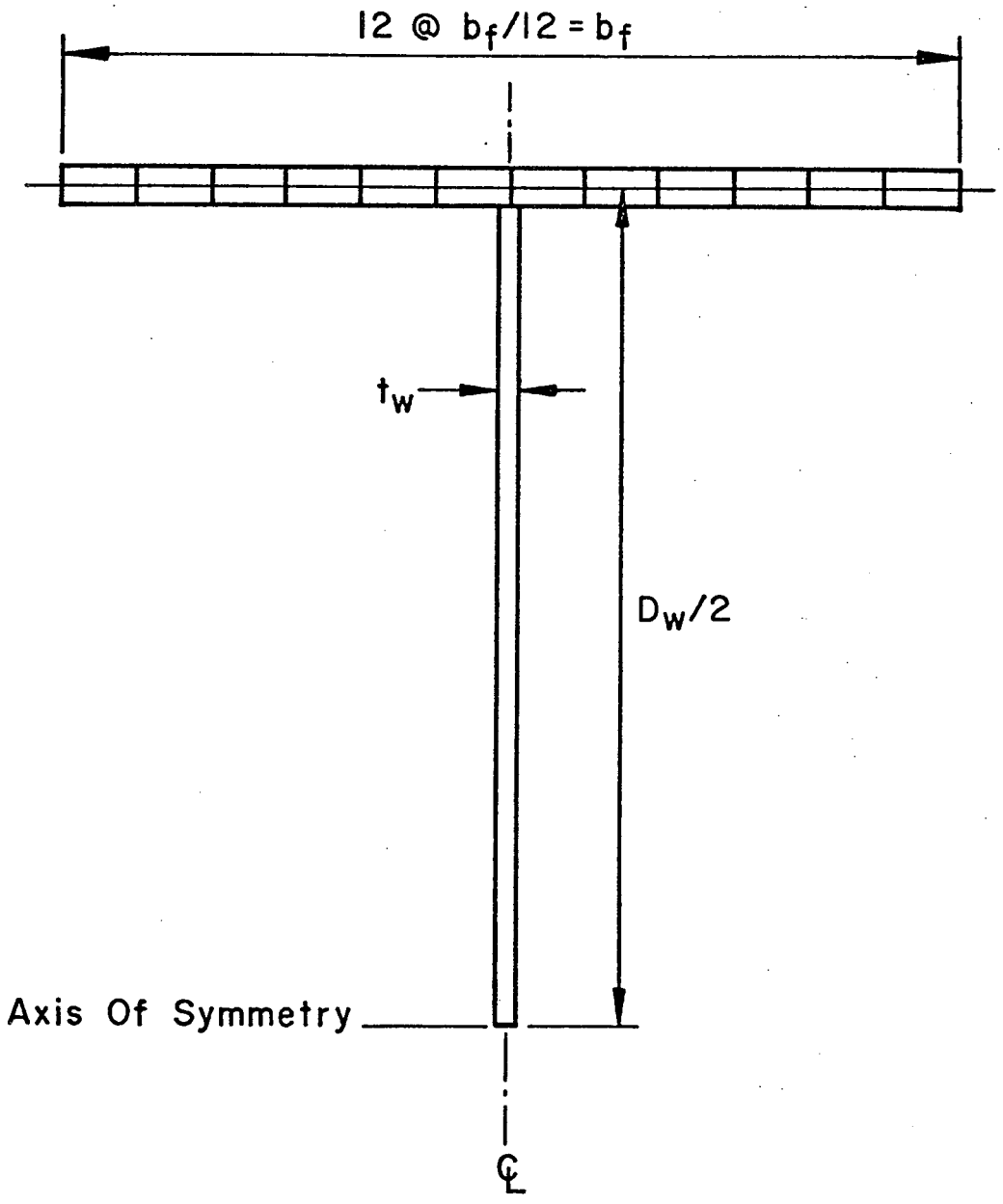

Element Stresses, Strains, And Temperatures Are Centroidal Values And Assumed Constant Over The Element.

Fig. 5 Model for Thermal Stress Analysis of Heat Curved Girders

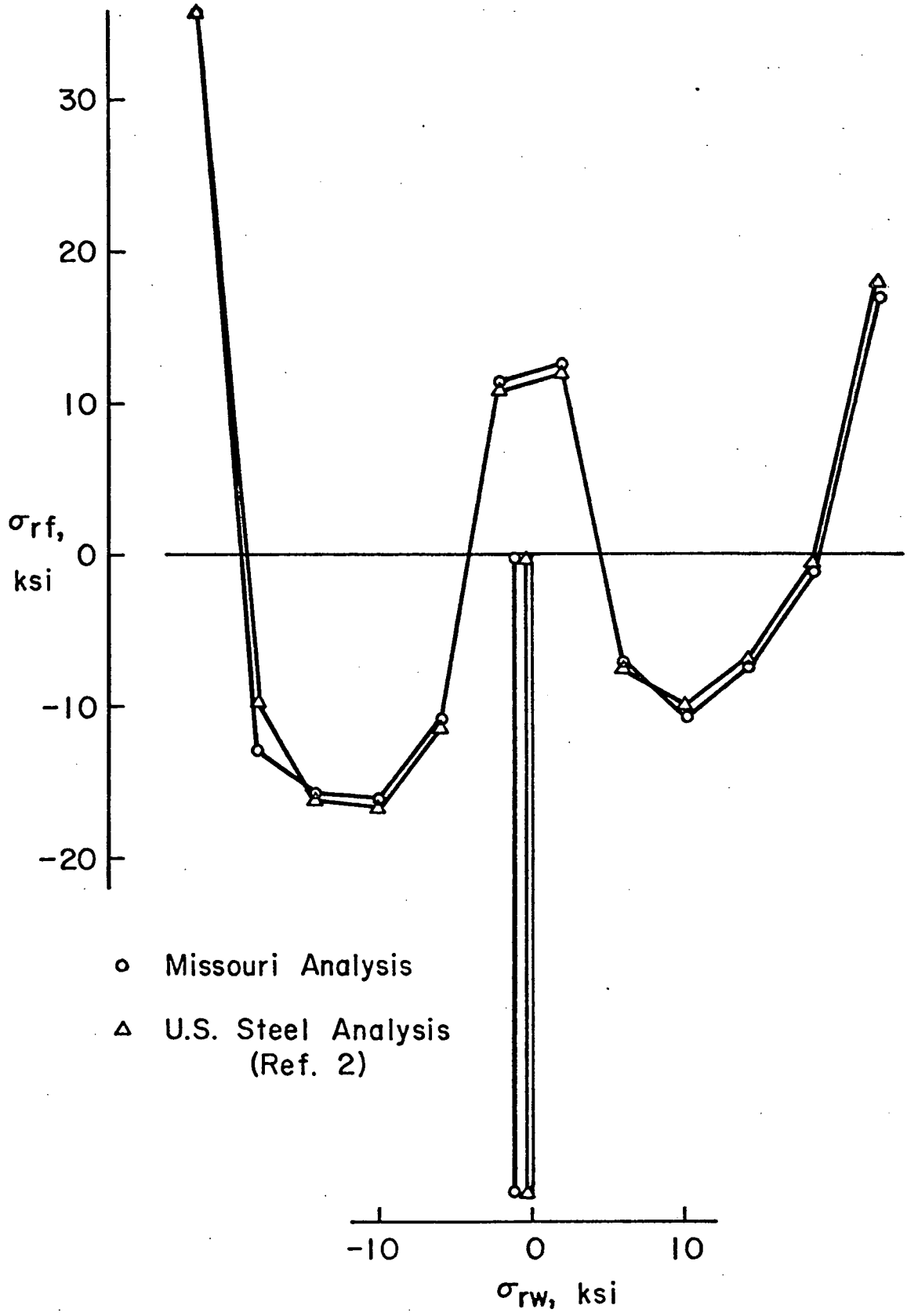

Fig. 6 Comparison of Final Residual Stresses due to Heat Curving as Given by Missouri and U.S. Steel Analysis

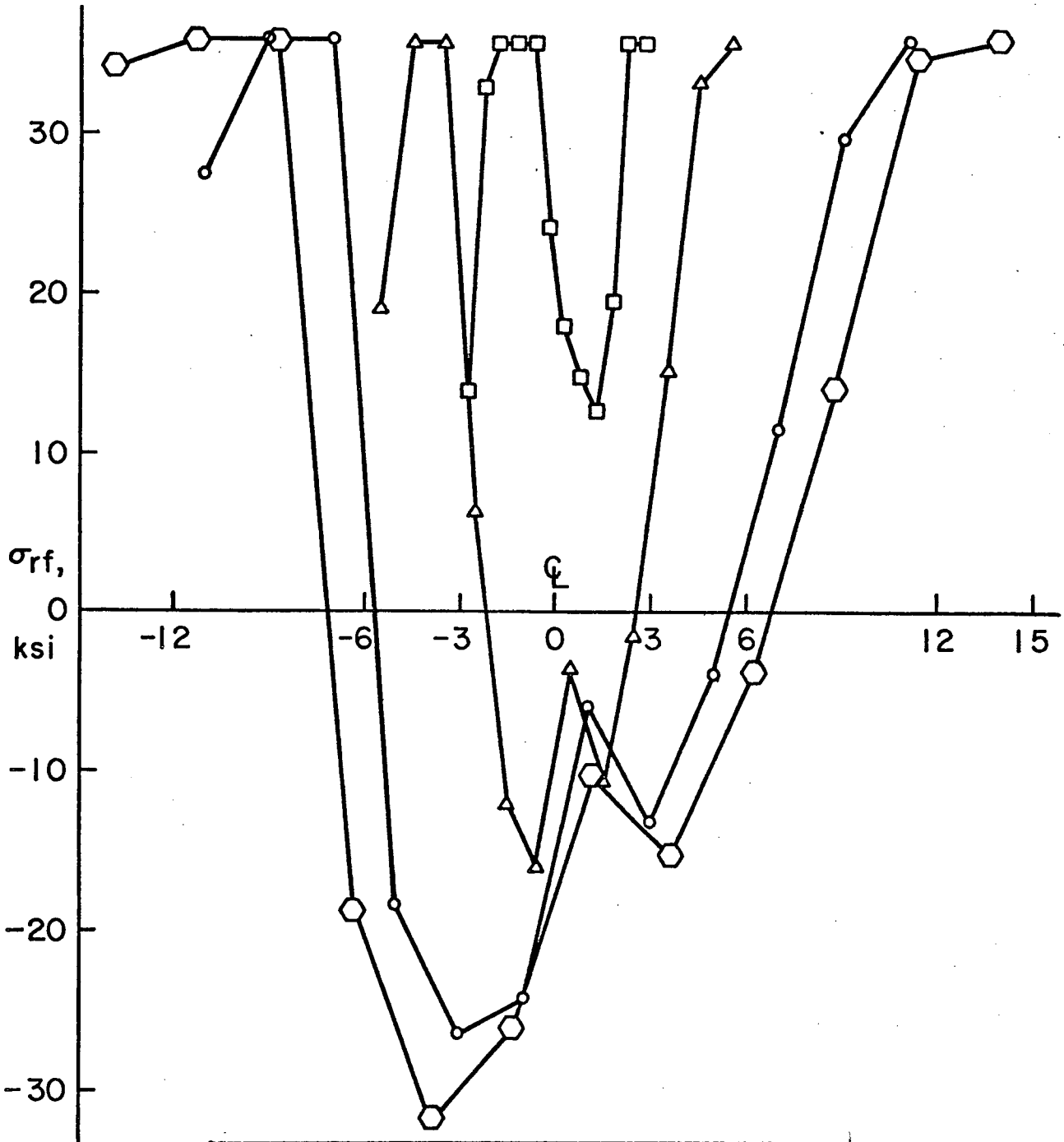

Symbol	Case	b_f	R	σ_{rw}
□	19	6	78.7	-21.1
△	20	12	190.2	-18.6
○	21	24	376.7	-22.9
⬡	22	30	3199.	-28.7

t_f = 2", D_w = 60", t_w = 0.5", σ_y = 36 ksi

b_h/b_f = 0.25, T_{max} = 1100°F

Fig. 7 Effect of b_f on Radius of Curvature and Residual Stresses

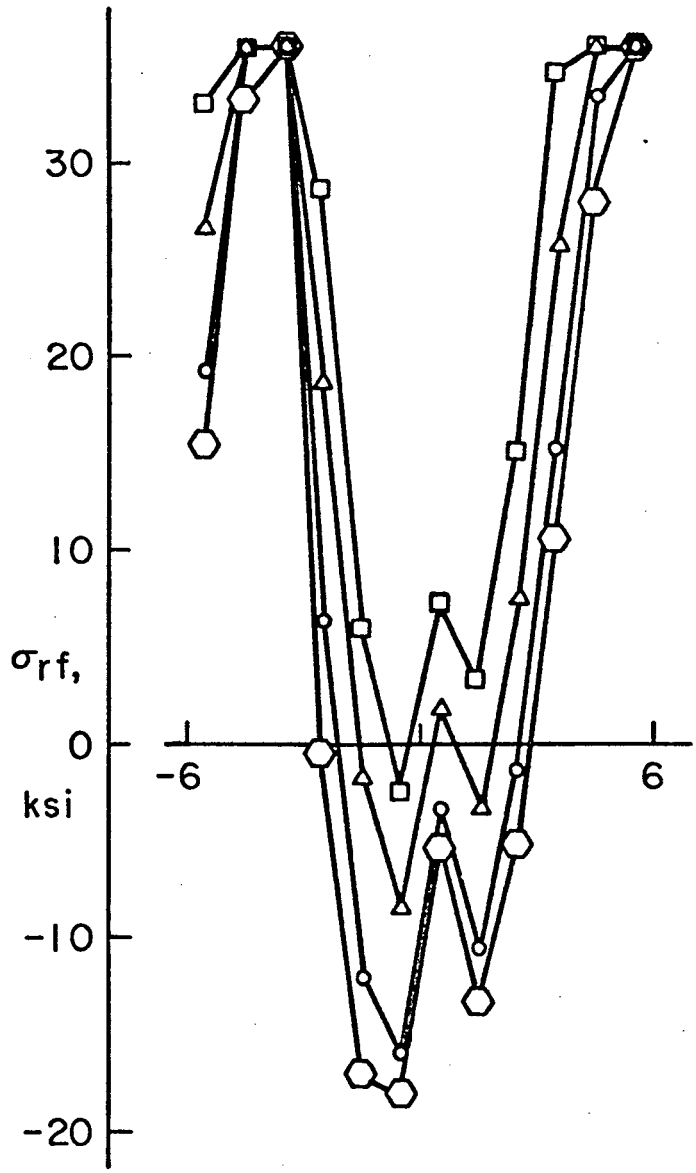

Symbol	Case	t_f	R	σ_{rw}
□	23	0.5	156.3	-9.0
△	24	1.0	168.5	-14.0
○	25	2.0	190.2	-18.6
⬡	26	3.0	204.4	-20.1

b_f = 12", D_w = 60", t_w = 0.5", σ_y = 36 ksi

b_h/b_f = 0.25, T_{max} = 1100°F

Fig. 8 Effect of t_f on Radius of Curvature and Residual Stresses

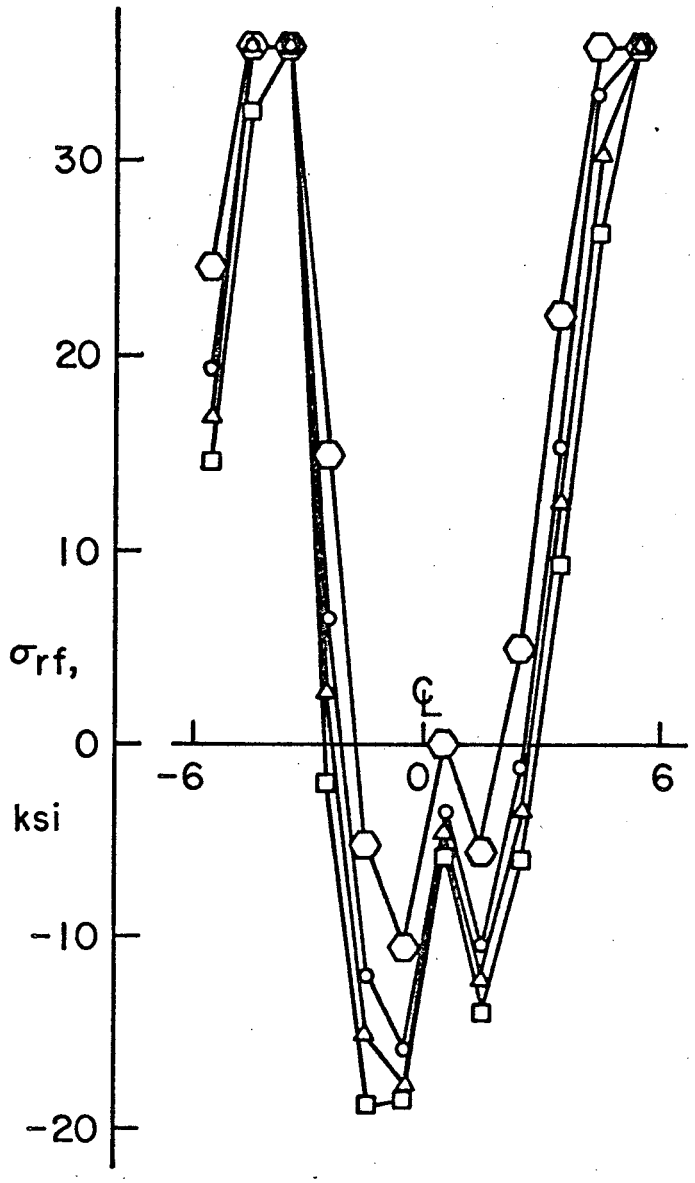

Symbol	Case	D_w	R	σ_{rw}
□	27	36	209.7	-20.2
△	28	48	197.8	-19.5
○	29	60	190.2	-18.6
⬡	30	96	174.4	-15.7

b_f = 12", t_f = 2", t_w = 0.5, σ_y = 36 ksi
b_h/b_f = 0.25, T_{max} = 110°F

Fig. 9 Effect of D_w on Radius of Curvature and Residual Stresses

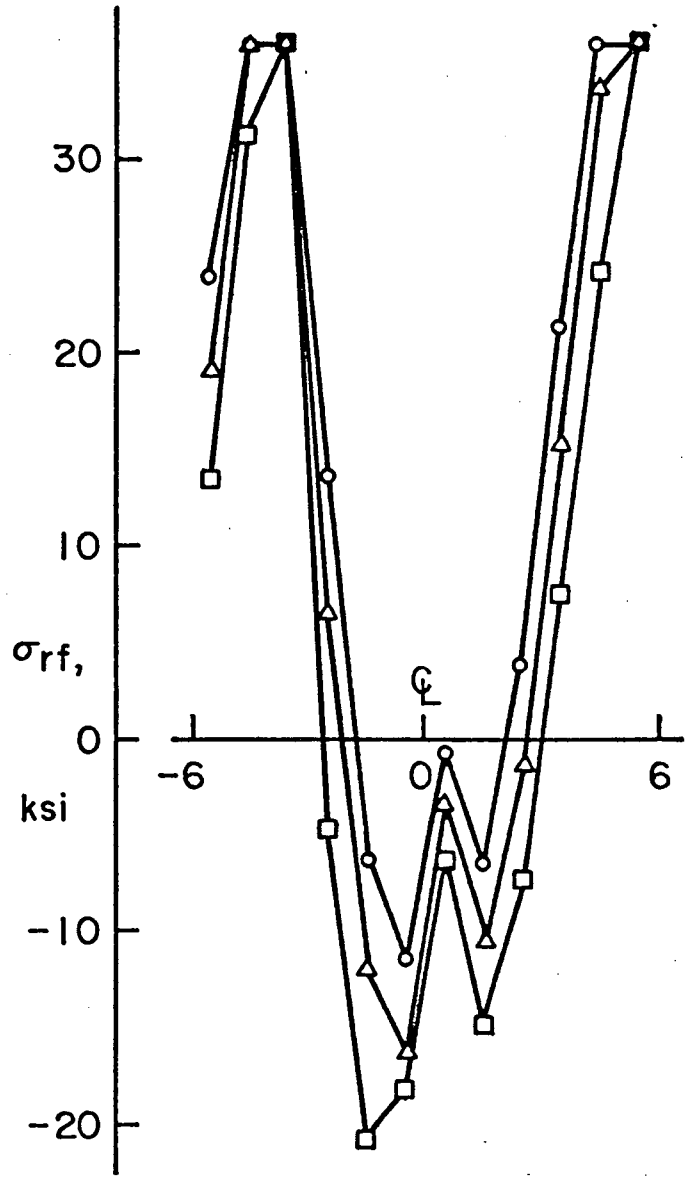

Symbol	Case	t_w	R	σ_{rw}
□	31	0.25	217.9	-20.6
△	32	0.50	190.2	-18.6
○	33	0.75	176.6	-16.2

b_f = 12", t_f = 2", D_w = 60", σ_y = 36ksi
b_h/b_f = 0.25, T_{max} = 1100°F

Fig. 10 Effect of t_w on Radius of Curvature and Residual Stresses

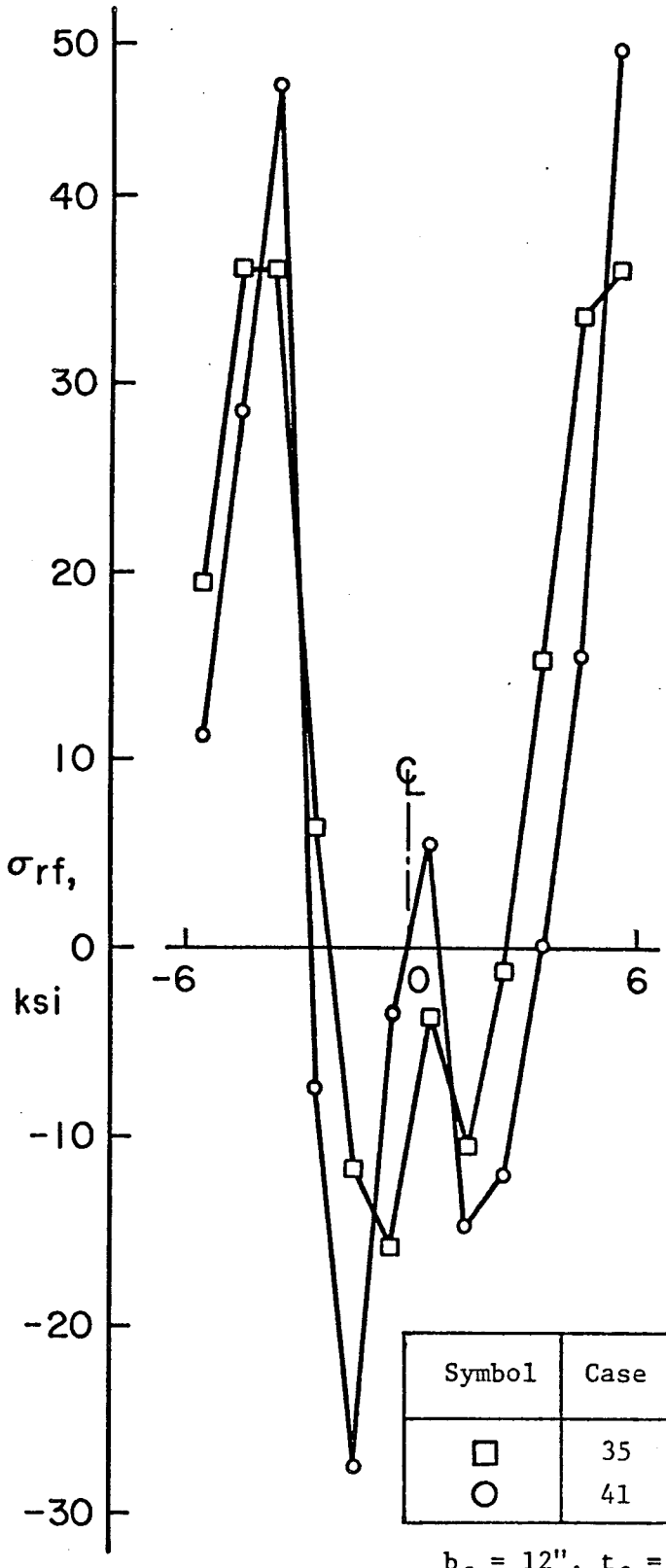

Symbol	Case	σ_y	R	σ_{rw}
□	35	36	190.2	-18.6
○	41	50	303.4	-11.8

$b_f = 12"$, $t_f = 2"$, $D_w = 60"$, $t_w = 0.5"$

$b_h/b_f = 0.25$, $T_{max} = 1100^oF$

Fig. 11 Effect of σ_y on Radius of Curvature and Residual Stresses

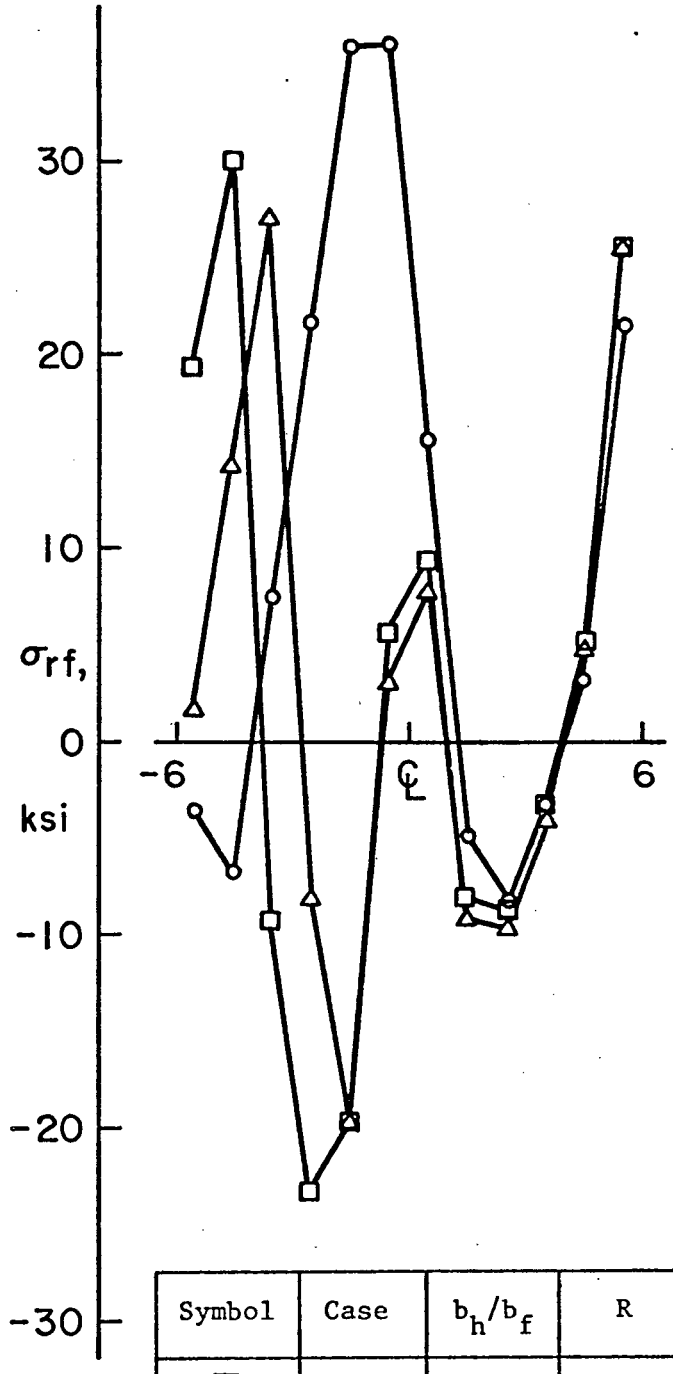

Symbol	Case	b_h/b_f	R	σ_{rw}
□	37	0.167	745.7	-3.0
△	38	0.250	690.4	-4.5
○	39	0.500	1985.	-15.3

b_f = 12", t_f = 2", D_w =60", t_w = 0.5"
σ_y = 36 ksi, T_{max} = 800°F

Fig. 12 Effect of b_h/b_f on Radius of Curvature and Residual Stresses

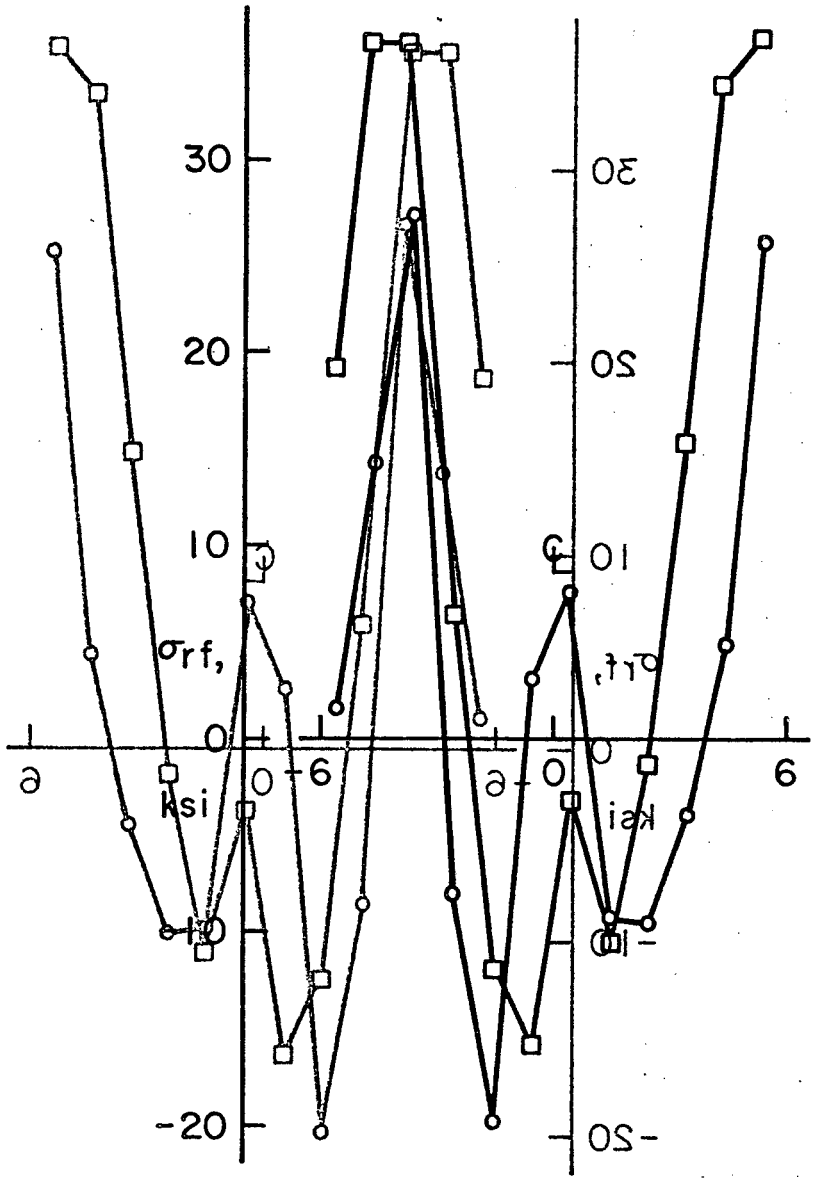

Symbol	Case	T_{max}	R	σ_{rw}
□	35	1100	190.2	-18.6
○	38	800	690.4	-4.5

b_f = 12", t_f = 2", D_w = 60", t_w = 0.5"

σ_y = 36 ksi, b_h/b_f = 0.25

Fig. 13 Effect of T_{max} on Radius of Curvature and Residual Stresses

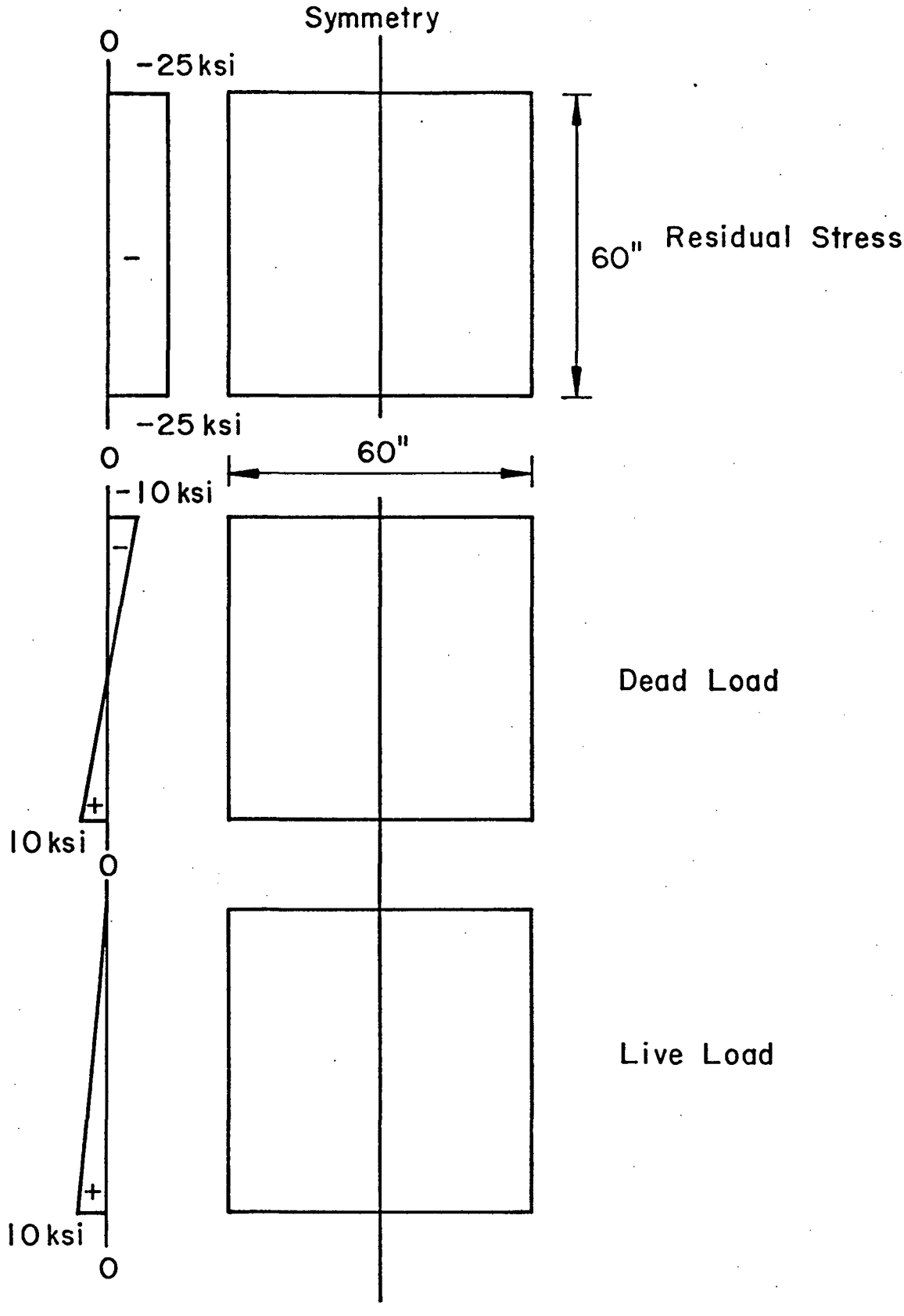

Fig. 14 Successive Load Cases for Web Boundary Study

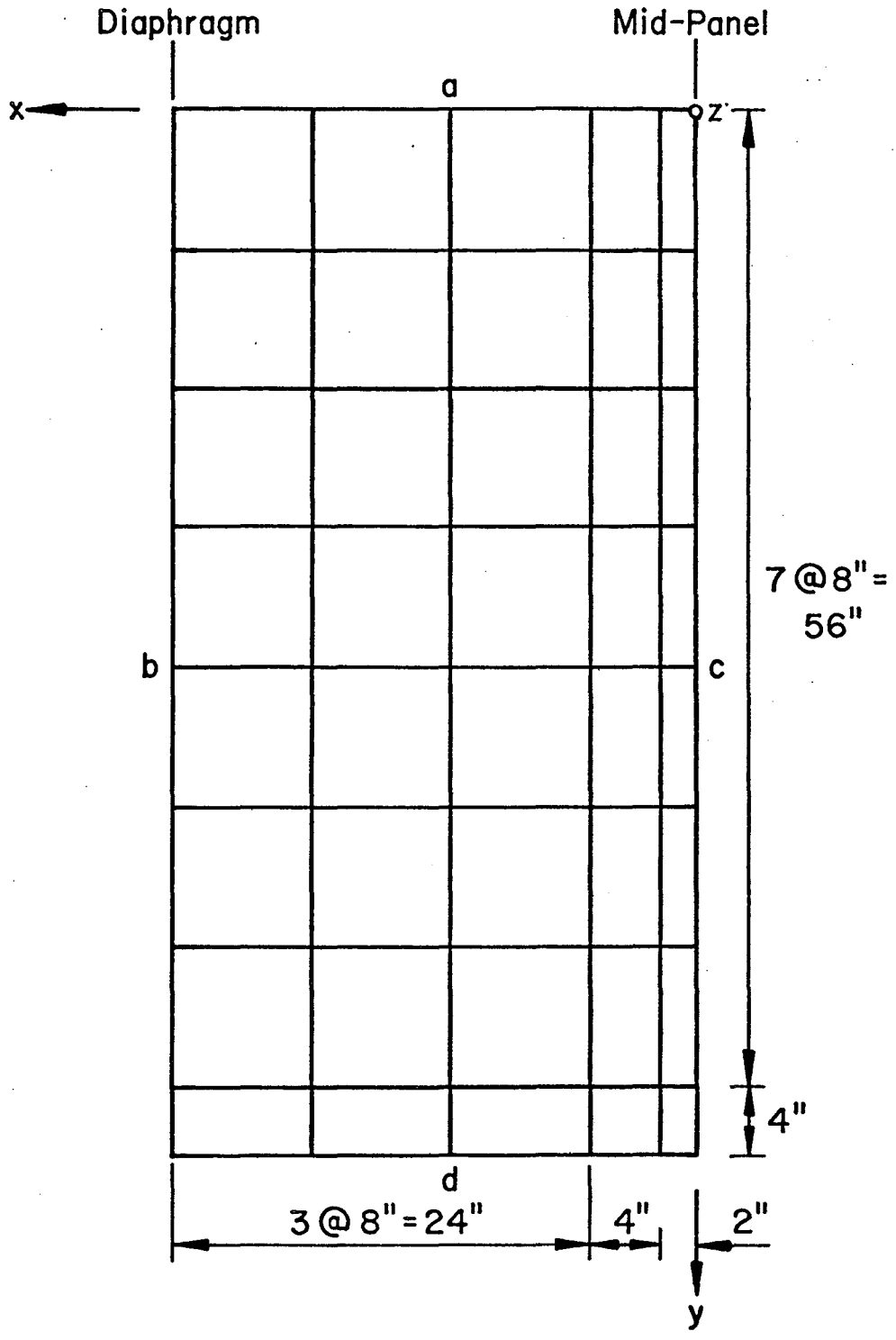

Boundary Conditions Along Sides a, b, c, And d Are Indicated In Table 5.

Fig. 15 Finite Element Discretization for Web Boundary Study

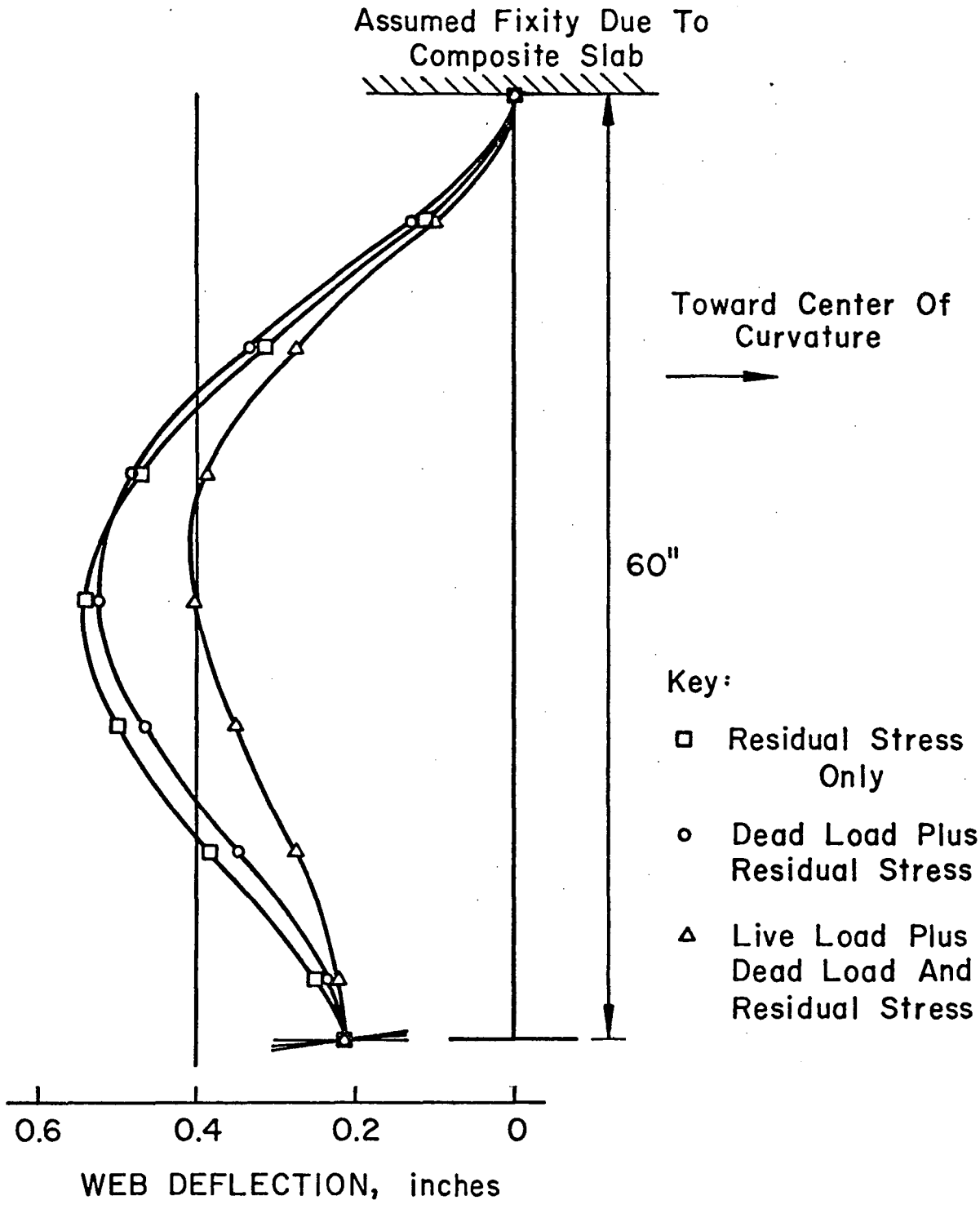

Fig. 16 Cumulative Web Deflection for Successive Load Cases - Run 4

8. APPENDIXES

APPENDIX A: Determination of Dimensionless Temperature Coefficients

As noted in Art. 2.1 the final residual stress distribution and radius of curvature due to heat curving are dependent upon the temperature distribution across the flange width throughout the heat-curving process. In this investigation the continuous variation of temperature during the heat-curving process is modeled by the instantaneous temperature at twelve points across the girder cross-section for six discrete time increments. Very little data is available on the actual distribution of temperature during heat curving, therefore, it is necessary to predict the required temperature distributions by a theoretical analysis.

The temperature at a given point on the girder cross-section for a given time increment is predicted by Eq. 2-1. The dimensionless temperature coefficient is determined by an analysis based on the principles of heat transfer in a thin, semi-infinite plate.

As an idealized point source of heat moves at constant velocity along the edge of a uniform, thin, semi-infinite plate a steady state of heat transfer develops. The general equation for the temperature distribution is:

$$T_{ij} = T_o + \frac{Q_p}{k} e^{-\lambda v \zeta} \frac{K_o(\lambda v r)}{h} \qquad (B\text{-}1)^{15,16}$$

where:

T_{ij} = the temperature at the point, i, at the time increment, t_j

T_o = the ambient temperature

Q_p = the total heat input

k = thermal conductivity

v = the velocity of the heat source

$\zeta = vt_j$ = the distance from the heat source to the cross-section of interest at the time increment, t_j

$r = \sqrt{\zeta^2 + y_i^2}$ where y_i is the distance from the edge of the plate to the point, i

$1/2\lambda = k/s\rho$ = thermal diffusivity

s = specific heat of the material

ρ = density of the material

K_o = modified Bessel function of the second kind, zero order, and

h = plate thickness

Comparison of Eq. 2-1 and B-1 shows that the dimensionless temperature coefficients, k_{ij}, may be expressed as:

$$k_{ij} = \frac{Q_p}{k \Delta T} e^{-\lambda v \zeta} \frac{K_o(\lambda v r)}{h} \qquad \text{(B-2)}$$

where:

ΔT = the difference between the ambient temperature and the maximum heat-curving temperature

At this point, several simplifying assumptions should be noted. First, the total heat input, Q_p, is assumed sufficient to bring the entire heated width, b_h, to the maximum heat-curving temperature, T_{max}. Thus, the necessity of determining the magnitude of Q_p is avoided. Second, the idealized heat source is assumed to move along a path which is $(b_h - b_f/12)$ from the heated edge of the flange.

The combined effect of these simplifications is to produce values of k_{ij} as shown in Fig. 3. Time increments, t_1 and t_6, refer to the reference states before and after heat curving for which all $k_{i1} = k_{i6} = 0$, and, therefore, all $T_{i1} = T_{i6} = T_o$. Time increment t_2 refers to the moment of heating the heated edge of the girder to the heat-curving temperature, while time increments t_3 through t_5 refer to succeeding intervals of time during the cooling of the girder. The values of k_{ij} shown were computed by dropping the constant terms of Eq. B-2 and dividing Eq. B-2 by the maximum k_{i2}. In algebraic terms:

$$k_{ij} = \frac{e^{-\lambda v \zeta} \; K_o(\lambda v r)}{(\max k_{i2})} \qquad \text{(B-3)}$$

The resulting values of k_{ij} give temperature distributions throughout the heat-curving process (Fig. 4) that agree very favorably with the limited information available.[2,6] This approach to the determination of the dimensionless temperature coefficients has the added advantage of being easily programmed and added to the computer program used for the thermal stress analyses (Art. 2.2).

APPENDIX B: List of Reports Produced under DOT-FH-11.8198

"Fatigue of Curved Steel Bridge Elements"

Daniels, J. H., Zettlemoyer, N. Abraham, D., and Batcheler, R. P.
ANALYSIS AND DESIGN OF PLATE GIRDER AND BOX GIRDER TEST ASSEMBLIES, DOT-FH-11.8198.1, September, 1976.

Zettlemoyer, N. and Fisher, J. W.
STRESS CONCENTRATION, STRESS RANGE GRADIENT AND PRINCIPAL STRESS EFFECTS ON FATIGUE LIFE, DOT-FH-11.8198.2, June, 1977.

Herbein, W. C. and Daniels, J. H.
FATIGUE TESTS OF CURVED PLATE GIRDER ASSEMBLIES, DOT-FH-11.8198.3, May, 1977.

Batcheler, R. P., and Daniels, J. H.
FATIGUE TESTS OF CURVED BOX GIRDER TEST ASSEMBLIES, DOT-FH-11.8198.4, (in preparation).

Batcheler, R. P., and Daniels, J. H.
EFFECT OF HEAT CURVING ON THE FATIGUE STRENGTH OF PLATE GIRDERS, DOT-FH-11.8198.5, August, 1977.

Abraham, D., Yen, B. T., and Daniels, J. H.
EFFECT OF INTERNAL DIAPHRAGMS ON THE FATIGUE STRENGTH OF CURVED BOX GIRDERS, DOT-FH-11.8198.6, (in preparation).

Daniels, J. H.
ULTIMATE STRENGTH TESTS OF CURVED PLATE GIRDER AND BOX GIRDER ASSEMBLIES, DOT-FH-11.8198.7, (in preparation).

Daniels, J. H., Fisher, J. W., and Yen, B. T.
DESIGN RECOMMENDATIONS FOR FATIGUE OF CURVED PLATE GIRDER AND BOX GIRDER BRIDGES, DOT-FH-11.8198.8, (in preparation).

9. ACKNOWLEDGMENTS

This study was conducted in the Department of Civil Engineering and Fritz Engineering Laboratory, under the auspices of the Lehigh University Office of Research, as a part of a research investigation sponsored by the Federal Highway Administration (FHWA) of the United States Department of Transportation. Dr. D. A. VanHorn is Chairman of the Department of Civil Engineering and Dr. L. S. Beedle is Director of Fritz Engineering Laboratory, Lehigh University.

The FHWA Manager is Mr. Jerar Nishanian. The contributions of the Lehigh Project Advisory Panel are gratefully acknowledged. The Advisory Panel members are Messers: A. P. Cole, C. G. Culver, R. S. Fountain, G. F. Fox, A. Lally and I. M. Viest.

The following members of the faculty and staff of Lehigh University made major contributions in the conduct of this work: Dr. J. W. Fisher, Dr. B. T. Yen, and Dr. N. Zettlemoyer.

The manuscript was typed by Ms. Shirley Matlock and Ms. Mary Snyder. The figures were prepared under the direction of John M. Gera. John Maurer assisted in assembling the manuscript.

10. REFERENCES

1. Thatcher, W. M.
   HORIZONTALLY CURVED GIRDERS - FABRICATION AND DESIGN, Engineering Journal, AISC, July, 1967.

2. Brockenbrough, R. L.
   THEORETICAL STRESSES AND STRAINS FROM HEAT CURVING, Journal of the Structural Division, ASCE, Vol. 96, No. ST7, July, 1970.

3. New York State Department of Transportation
   STEEL CONSTRUCTION MANUAL, Design and Construction Division, Albany, N. Y., August, 1973.

4. Brockenbrough, R. L.
   FABRICATION AIDS FOR CONTINUOUSLY HEAT-CURVED GIRDERS, United States Steel Corporation, Monroeville, Pa., April, 1972.

5. Brockenbrough, R. L.
   FABRICATION AIDS FOR GIRDERS CURVED WITH V-HEATS, United States Steel Corporation, Monroeville, Pa., January, 1973.

6. Brockenbrough, R. L., and Ives, K. D.
   EXPERIMENTAL STRESSES AND STRAINS FROM HEAT CURVING, Journal of the Structural Division, ASCE, Vol. 96, No. ST7, July, 1970.

7. Brockenbrough, R. L.
   CRITERIA FOR HEAT CURVING STEEL BEAMS AND GIRDERS, Journal of the Structural Division, ASCE, Vol. 96, No. ST10, Oct., 1970.

8. AASHO Subcommittee on Bridges and Structures
   STANDARD SPECIFICATIONS FOR HIGHWAY BRIDGES, AASHO, Eleventh Ed., Washington, D. C., 1973.

9. Daniels, J. H., Zettlemoyer, N., Abraham, D., and Batcheler, R. P.
   ANALYSIS AND DESIGN OF PLATE GIRDER AND BOX GIRDER TEST ASSEMBLIES, Fatigue of Curved Steel Bridge Elements, Report DOT-FH-11.8198.1, Federal Highway Administration, September, 1976.

10. Zettlemoyer, N. and Fisher, J. W.
    STRESS CONCENTRATION, STRESS RANGE GRADIENT AND PRINCIPAL STRESS EFFECTS ON FATIGUE LIFE, Fatigue of Curved Steel Bridge Elements, Report DOT-FH-11.8198.2, Federal Highway Administration, June, 1977.

11. Herbein, W. C. and Daniels, J. H.
    FATIGUE TESTS OF CURVED PLATE GIRDER ASSEMBLIES, Fatigue of Curved Steel Bridge Elements, Report DOT-FH-11.8198.3, Federal Highway Administration, May, 1977.

12. Batcheler, R. P., and Daniels, J. H.
FATIGUE TESTS OF CURVED BOX GIRDER TEST ASSEMBLIES, Fatigue of Curved Steel Bridge Elements, Report DOT-FH-11.8198.4, Federal Highway Administration (in preparation).

13. Abraham, D., Yen, B. T., and Daniels, J. H.
EFFECT OF INTERNAL DIAPHRAGMS ON THE FATIGUE STRENGTH OF CURVED BOX GIRDERS, Fatigue of Curved Steel Bridge Elements, Report DOT-FH-11.8198.6, Federal Highway Administration (in preparation).

14. Daniels, J. H., Fisher, J. W., and Yen, B. T.
DESIGN RECOMMENDATIONS FOR FATIGUE OF CURVED PLATE GIRDER AND BOX GIRDER BRIDGES, Fatigue of Curved Steel Bridge Elements, Report DOT-FH-11.8198.8, Federal Highway Administration (in preparation).

15. Tall, L.
RESIDUAL STRESSES IN WELDED PLATES - A THEORETICAL STUDY, Welding Journal, Vol. 43, AWS, January, 1964.

16. Myers, P. S., Uyehara, O. A., and Borman, G. L.
FUNDAMENTALS OF HEAT FLOW IN WELDING, Welding Research Council Bulletin, No. 123, July, 1967.

17. Doi, D., and Guell, D. L.
FLAME CAMBERING OF WIDE-FLANGE STEEL BEAMS - A DISCRETE METHOD OF THERMAL STRESS ANALYSIS APPLIED TO SIMPLE BEAMS, Permanent Deflections and Loss of Camber in Steel Bridge Beams, Vol. II, Appendix IV, University of Missouri, Columbia, Missouri.

18. Paris, P. C.
THE FRACTURE MECHANICS APPROACH TO FATIGUE, Fatigue - An Interdisciplinary Approach, Proceedings of the Tenth Sagamore Army Material Research Conference, Syracuse University Press, 1964.

19. Wei, R. P.
FRACTURE MECHANICS APPROACH TO FATIGUE ANALYSIS IN DESIGN, Applications of Fracture Mechanics to Engineering Problems, Report IFSM-72-23, Institute of Fracture and Solid Mechanics, Lehigh University, Bethlehem, Pa., November, 1972.

20. Zettlemoyer, N.
STRESS CONCENTRATION AND FATIGUE OF WELDED DETAILS, Dissertation presented to Lehigh University at Bethlehem, Pa., October, 1976. Available from University Microfilms, Inc., Ann Arbor, Mich.

21. Fisher, J. W., Frank, K. H., Hirt, M. A., and McNamee, B. M.
EFFECT OF WELDMENTS ON THE FATIGUE STRENGTH OF STEEL BEAMS, NCHRP Report No. 102, Highway Research Board, National Academy of Sciences - National Research Council, Washington, D. C., 1970.

22. Fisher, J. W., Albrecht, P. A., Yen, B. T., Klingerman, D. J., and McNamee, B. M.
FATIGUE STRENGTH OF STEEL BEAMS WITH WELDED STIFFENERS AND ATTACHMENTS, NCHRP Report No. 147, Transportation Research Board, National Research Council, Washington, D. C., 1974.

23. Gurney, T. R. and Maddox, S. J.
A RE-ANALYSIS OF FATIGUE DATA FOR WELDED JOINTS IN STEEL, Welding Research International, Vol. 3, No. 4, 1973.

24. Fisher, J. W. and Gurney, T. R.
HIGH-CYCLE FATIGUE OF CONNECTIONS AND DETAILS, Proceedings of the International Conference on the Planning and Design of Tall Buildings, ASCE-IABSE, Lehigh University, Bethlehem, Pa., August, 1972.

25. Nelson, D. V. and Fuchs, H. O.
PREDICTION OF FATIGUE CRACK GROWTH UNDER IRREGULAR LOADING, Fatigue Crack Growth under Spectrum Loads, ASTM STP 595, Philadelphia, Pa., 1976.

26. Barsom, J. M.
FATIGUE CRACK GROWTH UNDER VARIABLE AMPLITUDE LOADING IN VARIOUS BRIDGE STEELS, Fatigue Crack Growth under Spectrum Loads, ASTM STP 595, Philadelphia, 1976.

27. Mueller, J. A., and Yen, B. T.
GIRDER WEB BOUNDARY STRESSES AND FATIGUE, Welding Research Council Bulletin, No. 127, January, 1968.

28. Bathe, K. J., Wilson, E. L., and Peterson, F. E.
SAP IV - STRUCTURAL ANALYSIS PROGRAM FOR THE STATIC AND DYNAMIC RESPONSE OF LINEAR SYSTEMS, Report EERC-73-11, University of California, Berkeley, California, April, 1974.

29. Fisher, J. W.
GUIDE TO 1974 AASHTO FATIGUE SPECIFICATIONS, AISC, New York, N. Y., 1974.

30. Galambos, C. F., and Heins, C. P.
LOADING HISTORY OF HIGHWAY BRIDGES: COMPARISON OF STRESS RANGE HISTOGRAMS, Highway Research Record, No. 354, Highway Research Board, 1971.

31. American Welding Society
STRUCTURAL WELDING CODE, AWS Structural Welding Committee, AWS D1.1-75, 1975.